

6-2023

## **PREDICTIVE ABILITY OF A 3D BODY SCANNING MOBILE APPLICATION FOR METABOLIC HEALTH RISK**

Caleb Brandner

Follow this and additional works at: [https://aquila.usm.edu/masters\\_theses](https://aquila.usm.edu/masters_theses)



Part of the [Exercise Science Commons](#), and the [Telemedicine Commons](#)

---

### **Recommended Citation**

Brandner, Caleb, "PREDICTIVE ABILITY OF A 3D BODY SCANNING MOBILE APPLICATION FOR METABOLIC HEALTH RISK" (2023). *Master's Theses*. 983.

[https://aquila.usm.edu/masters\\_theses/983](https://aquila.usm.edu/masters_theses/983)

This Masters Thesis is brought to you for free and open access by The Aquila Digital Community. It has been accepted for inclusion in Master's Theses by an authorized administrator of The Aquila Digital Community. For more information, please contact [aquilastaff@usm.edu](mailto:aquilastaff@usm.edu).

Summer 6-12-2023

## **PREDICTIVE ABILITY OF A 3D BODY SCANNING MOBILE APPLICATION FOR METABOLIC HEALTH RISK**

Caleb Brandner

Follow this and additional works at: [https://aquila.usm.edu/masters\\_theses](https://aquila.usm.edu/masters_theses)



Part of the [Exercise Science Commons](#), and the [Telemedicine Commons](#)

---

### **Recommended Citation**

Brandner, Caleb, "PREDICTIVE ABILITY OF A 3D BODY SCANNING MOBILE APPLICATION FOR METABOLIC HEALTH RISK" (2023). *Master's Theses*. 983.

[https://aquila.usm.edu/masters\\_theses/983](https://aquila.usm.edu/masters_theses/983)

This Masters Thesis is brought to you for free and open access by The Aquila Digital Community. It has been accepted for inclusion in Master's Theses by an authorized administrator of The Aquila Digital Community. For more information, please contact [aquilastaff@usm.edu](mailto:aquilastaff@usm.edu).

PREDICTIVE ABILITY OF A 3D BODY SCANNING MOBILE APPLICATION FOR  
METABOLIC HEALTH RISK

by

Caleb Brandner

A Thesis

Submitted to the Graduate School,  
the College of Education and Human Sciences  
and the School of Kinesiology and Nutrition  
at The University of Southern Mississippi  
in Partial Fulfillment of the Requirements  
for the Degree of Master of Science

Approved by:

Dr. Austin Graybeal, Committee Chair

Dr. Jon Stavres

Dr. Riley Galloway

Dr. Stephanie McCoy

August 2023

COPYRIGHT BY

Caleb Brandner

2023

*Published by the Graduate School*



## ABSTRACT

There is an increasing prevalence of obesity within the US and rising rates of metabolic syndrome among those aged 20-39 concurrent with a decrease in the reception of primary care. Limitations to healthcare including access, cost, and availability, highlighting the need for simple, efficient, and accessible cardiometabolic health risk screening. Given the surge in smartphone ownership over the last decade, this study sought to determine the predictive ability of a mobile 3D-optical (3DO) body composition assessment application in determining metabolic health risk. A total of 62 participants (female: 36) underwent traditional anthropometric measurements, 3DO body scanning using a smartphone application, and the collection of chronic health biomarkers from capillary blood. Metabolic syndrome risk scores (MSs) were determined using previously generated sex- and race/ethnicity-specific equations. Three prediction models were produced using variables extracted from the 3DO scans (anthropometric, body composition, and combined models), with the final models produced by backwards regression. Sex specific models were also generated. The combined model including both body composition and anthropometric variables provided the strongest predictor of MSs ( $R^2 = 0.64$ ,  $p < 0.001$ ), with performance improving when separated into female ( $R^2 = 0.77$ ,  $p < 0.001$ ) and male specific models ( $R^2 = 0.87$ ,  $p = 0.002$ ). The combined sex-specific models did not reveal significant proportional biases (female: coefficient = 0.138,  $p = 0.123$ , male: coefficient = -0.072,  $p = 0.142$ ). The findings of this study provide preliminary evidence for the use of mobile 3DO scanning for cardiometabolic health risk screening. Thus, mobile 3DO scanning may provide an affordable, accessible, and easy to use tool that can be deployed remotely to improve healthcare access.

## ACKNOWLEDGMENTS

I'm extremely grateful to my advisor, Dr. Austin Graybeal, for his invaluable guidance, expertise, and continuous encouragement throughout the research process. The faculty members, Dr. Jon Stavres, Dr. Stephanie McCoy, and Dr. Riley Galloway, for their insights and input that guided and improved the quality of this work. The undergraduate assistants, Havens Wise and Alex Henderson, for their hard work and assistance throughout the data collection process.

## DEDICATION

I would like to dedicate this thesis to my loving family, especially my parents, Allan and Katrina, whose unwavering support, hours on the phone, and constant encouragement have been instrumental in my academic journey. Their prayers, support, and belief in me have provided the foundation needed to thrive throughout this challenging endeavor. This thesis is also dedicated to my close friends, especially Nick, Joe, Peter, and Robert, who have been a source of inspiration, motivation, and have strengthened me throughout this challenging endeavor. To my family and friends, thank you for your faith, your prayers, and the love you have shown me. Your presence in my life has made all the difference and has been a constant reminder of the presence and love of Jesus Christ. I dedicate this thesis to each and every one of you with heartfelt love and appreciation.

TABLE OF CONTENTS

ABSTRACT ..... ii

ACKNOWLEDGMENTS ..... iii

DEDICATION ..... iv

LIST OF TABLES ..... vii

LIST OF ABBREVIATIONS ..... viii

CHAPTER I - INTRODUCTION ..... 1

CHAPTER II - LITERATURE REVIEW ..... 8

    2.1 Obesity and Metabolic Syndrome ..... 8

    2.2 Body Composition ..... 18

    2.3 Smartphone 3D Body Scanning Applications ..... 25

CHAPTER III - Methods ..... 29

    3.1 Participants ..... 29

    3.2 Procedures ..... 29

    3.3 Mobile 3-Dimensional Imaging Analysis ..... 30

    3.4 Metabolic Health Assessment ..... 31

    3.5 Metabolic Health Risk Score ..... 32

    3.6 Prediction Modelling ..... 33

    3.7 Statistical Analyses ..... 33

CHAPTER IV - RESULTS ..... 35



4.1 Participants.....	35
4.2 Precision Analyses .....	36
4.3 Body Composition Models .....	36
4.4 Anthropometric Models .....	36
4.5 Combined Models.....	37
4.6 Prediction Equation Agreement Analysis.....	39
CHAPTER V – DISCUSSION.....	45
APPENDIX A – IRB Approval Letter.....	55
REFERENCES .....	56

## LIST OF TABLES

<b>Table 4.1</b> Physical characteristics of study participants.....	35
<b>Table 4.2</b> Body composition model summary .....	36
<b>Table 4.3</b> Anthropometric model summary .....	37
<b>Table 4.4</b> Combined models summary.....	38

## LIST OF ABBREVIATIONS

<i>3DO</i>	three-dimensional optical
<i>AC</i>	upper arm circumference
<i>ADP</i>	air displacement plethysmography
<i>BF%</i>	body fat percent
<i>BGAs</i>	blood gas analyzers
<i>BIA</i>	bioelectrical impedance analysis
<i>BIS</i>	bioelectrical impedance spectroscopy
<i>BMC</i>	bone mineral content
<i>BMI</i>	body mass index
<i>BP</i>	blood pressure
<i>BSA</i>	body surface area
<i>CAD</i>	coronary artery disease
<i>CC</i>	calf circumference
<i>ChC</i>	chest circumference
<i>CT</i>	computed tomography
<i>CVD</i>	cardiovascular disease
<i>DXA</i>	dual energy x-ray absorptiometry
<i>EE</i>	energy expenditure
<i>FBG</i>	fasting blood glucose
<i>FC</i>	forearm circumference
<i>FFM</i>	fat-free mass
<i>FFMI</i>	fat-free mass index

<i>FM</i>	fat mass
<i>FMI</i>	fat mass index
<i>HC</i>	hip circumference
<i>HDL</i>	high density lipoprotein
<i>HW</i>	hydrostatic weighing
<i>ICC</i>	intraclass correlation coefficients\
<i>LDL</i>	low-density lipoprotein
<i>M-3DO</i>	mobile three-dimensional optical
<i>MetS</i>	metabolic syndrome
<i>MFBLA</i>	multi-frequency BIA
<i>MRI</i>	magnetic resonance imaging
<i>MSE</i>	mean square error
<i>MSs</i>	metabolic risk score
<i>PA</i>	physical activity
<i>PAD</i>	peripheral arterial disease
<i>PE</i>	precision error
<i>SC</i>	stomach circumference
<i>SES</i>	socioeconomic status
<i>SKF</i>	skinfold
<i>SW</i>	shoulder width
<i>T2D</i>	type 2 diabetes
<i>TC</i>	thigh circumference
<i>TDEE</i>	total daily energy expenditure

<i>TG</i>	triglycerides
<i>VAT</i>	visceral adipose tissue
<i>WC</i>	waist circumference
<i>WHR</i>	waist-to-hip ratio
<i>WHt</i>	waist-to-height ratio

## CHAPTER I - INTRODUCTION

Obesity is defined as the excessive accumulation and storage of body fat and is traditionally classified by the relationship between body mass in kilograms and height in meters squared (a.k.a. body mass index [BMI],  $\text{kg}/\text{m}^2$ ). According to the National Institutes of Health, an individual with a BMI of  $30 \text{ kg}/\text{m}^2$  or greater is categorized as having obesity<sup>1</sup>, which poses a significant health risk. In fact, each additional  $5 \text{ kg}/\text{m}^2$  increase in BMI beyond  $25 \text{ kg}/\text{m}^2$  is associated with a 30% increase in mortality risk<sup>2</sup>. There exists strong associations between obesity and type II diabetes (T2D), hypertension, dyslipidemia, heart disease, cerebrovascular disease, and respiratory disease, gastrointestinal complications, osteoarthritis, and some cancers<sup>3</sup>, making it a significant public health issue. Though the health risks associated with excessive body fat are well established in public health discourse, knowledge of the risks associated with obesity has done little to mitigate its prevalence.

As of 2017-2018, 42.4% of US adults had a BMI classification of obese, an increase of 11.9% from 1999-2000<sup>4</sup>. The increasing prevalence of obesity presents not only a public health risk, but a burden on medical spending. For individuals with obesity, annual medical spending costs an average of \$2,505 more when compared to individuals classified as normal weight, and costs as much as \$260.6 billion per year in annual medical spending in the US<sup>5</sup>. BMI has been well validated for its role as an indicator of excess body fat<sup>6</sup> making it a useful tool, but healthcare providers are not utilizing the information to address the growing obesity epidemic<sup>7</sup>. Yet, BMI may not accurately demonstrate the full picture of one's metabolic health risk and more information is necessary to determine one's health status<sup>8,9</sup>.

Of particular concern with the presence of obesity is the potential development of metabolic syndrome (MetS). MetS is characterized by abdominal obesity, hypertension, dyslipidemia, and impaired fasting glucose<sup>10</sup>, and is considered present if an individual has three or more of the following risk factors; high blood pressure (BP) (>130/85 mmHg), high fasting blood glucose (FBG; >100 mg/dL), a waist circumference (WC) over 101.6 cm (men) or 88.9 cm (women), high fasting triglyceride (TG) levels (>150 mg/dL), and low fasting high-density lipoprotein (HDL) cholesterol levels (<40 mg/dl for men, <50 mg/dL for women)<sup>11</sup>. Prevalence of MetS in the US from 2015-2016 was 34.7% and though the overall increase in incidence was not significantly higher than previous years, there is a growing prevalence among those aged 20-39 years. From 2015-2016, prevalence among those aged 20-39 was 21.3%, those aged 40-59 was 42%, and those aged  $\geq 60$  was 50.4%, indicating a trend for increasing incidence of MetS with increasing age<sup>12</sup>.

Many methodologies currently exist to aid in the assessment and quantification of obesity and metabolic disease risk. While BMI provides limited information, it is one of the most widely used assessments for obesity and has been positively associated with systolic and diastolic BP, strongly positively associated with ischemic heart disease, and positively associated with stroke in middle aged individuals<sup>2</sup>. The higher the BMI the higher risk of coronary heart disease, stroke, cardiovascular disease (CVD), T2D, and all cause mortality<sup>13</sup>. Patient height and weight are often measured during normal physician visits and can be used for BMI calculations, but circumference measures such WC, hip circumference (HC) and waist-to-hip ratio (WHR), which may provide useful

information associated with metabolic health risk, are rarely collected during routine visits.

Waist-related metrics can be utilized for predicting cardiovascular disease mortality<sup>14</sup>, obesity risk<sup>15</sup>, truncal adiposity, and metabolic complications<sup>16,8</sup> and are strong and independent predictors of T2D<sup>17</sup>. The calculation of WHR demonstrates relative waist size and shows high correlation to fat mass (FM) around the viscera and abdominal organs<sup>18</sup>, and WC alone is an independent predictor of mortality<sup>19</sup>. As individual measures, taking both WC and HC measures together may provide a more robust understanding of mortality risk by providing measures of both upper- and lower-body adiposity<sup>20</sup>. Specifically, the excessive accumulation of visceral adipose tissue (VAT) is a component of abdominal obesity and is associated with a higher mortality risk than BMI-defined obesity<sup>21</sup> alone and has been implicated for its role in the development of insulin resistance<sup>22</sup>. Excess VAT may indicate dysfunctional lipid metabolism and increase the risk of hypertension, T2D, insulin resistance, stroke, inflammation, and dyslipidemia<sup>23</sup>.

While circumference measures have the potential to serve as valuable assessment tools, the use of a tape measure requires accurate and consistent landmarking for measurement sites and is thus subject to variance in reliability across observers<sup>24</sup>. Even with reliable measurements of body circumference and BMI, these simplistic measures are limited by their superficial nature, which are more aligned with size and stature, and may not accurately reveal body tissue compositions associated with disease. Utilizing body fat percent (BF%) cutoff points of  $\geq 25\%$  for men and  $\geq 35\%$  for females, Peltz et al. observed that BMI failed to categorize 46.2% of men and 50.7% of women that were



identified as having obesity when utilizing BF% as assessed by bioelectrical impedance analysis (BIA)<sup>25</sup>. Utilizing the same BF% cutoff points, Frankenfield et al. noted similar discrepancies between BMI and BIA BF% assessments with 30% of men and 46% of women with BMIs below 30kg/m<sup>2</sup> having a BF% above the obesity cutoff<sup>26</sup>, though it should be noted there are no conventional cutoffs for BF%. The presence of low fat-free mass (FFM) and high body fat that is descriptive of individuals with normal weight obesity has been implicated in the development of insulin resistance<sup>11,27,28</sup> and endothelial dysfunction<sup>11,29</sup>. The risks associated with high BF% and low FFM highlight the important roles that both adiposity and lean tissue can have in regulating health status and indicates that direct measures of body composition may be needed for a more thorough screening of metabolic health risk.

The most accurate methods of assessing body composition are computed tomography (CT) and magnetic resonance imaging (MRI). MRI scans must use section-by-section scanning in order to achieve full body analysis, which is time consuming, expensive, and may not be feasible for patients with claustrophobia due to the confined space of the scanner. CT scans are based on X-ray which requires the subject to be exposed to a substantial amount of radiation. Due to the limitations of MRI and CT, dual-energy x-ray absorptiometry (DXA) is often utilized as the criterion single device body composition measure. DXA is noninvasive and can be completed quickly, and unlike CT, the X-ray exposure is minimal. Despite this, DXA scans are not widely available and can be expensive to access for body composition assessments.

Bioelectrical impedance analysis (BIA) and bioelectrical spectroscopy (BIS) are additional non-invasive body composition technologies. Most traditional bioelectrical

impedance devices produce an electrical current which is sent through the body and estimates body composition from tissue impedance measurements (resistance and reactance). However, given the influence of cellular hydration status on body composition estimates assessed by this method, pre-test standardization remains a major limitation of BIA and BIS devices. As such, participants are required to be fasted and in a state of euhydration, where failure to adhere can result in meaningful changes in FM, FFM, and BF% values<sup>30</sup>. Further, differences exist in agreement between some single- and multi-frequency BIA (MFBIA) devices and BIS<sup>31,32</sup>. The variance in available technology limits the utility of the technology in clinical settings, highlighting the need for reliable non-invasive body composition and anthropometric assessment technology.

Three-dimensional body surface scanning is a new technology that has the potential to provide both easily accessible anthropometric and body composition assessments. Three-dimensional scanners commonly deploy one of two technologies for data acquisition; 1) structured light scanners which emit infrared light patterns across the surface of an object and measures light deformation of the pattern to produce a depth image; or 2) time-of-flight scanners which utilize visible light or infrared light and calculates “round trip time” for photons moving from the image sensor to the object and back to the camera to calculate depth<sup>33,34</sup>. The depth data collected from the scanner sensors are used to generate surface shape and cloud points of digital data (3D mesh/avatar) which can be used for circumference measurements, linear dimensions, and anatomical volumes, from which proprietary software can estimate body composition<sup>33</sup>. Three-dimensional optical (3DO) scanning devices have been validated against a four-compartment criterion model for assessment of BF%, demonstrating reliable estimates

with minor variance between devices<sup>35</sup>. 3DO scanning has demonstrated associations with VAT measurements from DXA and has shown significant correlations to specific biomarkers of metabolic health, such as HDL cholesterol, TG, glucose, insulin, and homeostatic model assessment of insulin resistance, making it a useful tool for monitoring metabolic health<sup>36</sup>.

Recently, 3DO smartphone applications have been developed that utilize two-dimensional photographs to estimate BF% and anthropometric data and has been validated against DXA for BF%<sup>37</sup>. Mobile 3DO (M-3DO) scanning presents an opportunity to collect user health information quickly, easily, and remotely at a low cost and without the need for technical expertise and in turn, improve access to metabolic health screening. With 85% of US adults reporting ownership of a smartphone as of 2020<sup>38</sup> and a 41% growth in full or partial telehealth utilization in US hospitals from 2010 to 2017<sup>39</sup>, the further development and validation of mobile health assessment techniques may expand the scope and accessibility of mobile healthcare. Telemedicine programs have been utilized to manage diabetes care<sup>40</sup>, provide mental health interventions<sup>41</sup>, and chronic disease lifestyle improvement<sup>42</sup>, yet the utilization of smartphone technology for anthropometric assessments and metabolic disease risk screening has not been done. Therefore, the purpose of this thesis is to assess the predictive power of a commercially available 3DO scanning application to assess metabolic health risk. This information would have significant implications for improving what is possible with telemedicine and providing remote health risk screening. With an increasing prevalence of obesity in rural regions<sup>43</sup> and among individuals of low socioeconomic status (SES)<sup>44,45</sup>, healthcare access is imperative. It is hypothesized that

measurements obtained with 3DO scanning will correlate to MetS risk factors, thus providing a viable option for at-home health risk screening.

## CHAPTER II - LITERATURE REVIEW

### 2.1 Obesity and Metabolic Syndrome

Obesity refers to the excessive accumulation of adipose tissue which is a product of chronic high energy intake and insufficient physical activity (PA) and is associated with several negative health outcomes<sup>1</sup>. This occurrence is dictated by the laws of thermodynamics, specifically the law of conservation of energy, where a positive shift in energy balance, defined as the rate of energy intake to the rate of energy output, will result in changes in body weight. Total daily energy expenditure (TDEE) can be broken down into three different components; resting metabolic rate, which is the energy required while lying supine, motionless, and awake; thermic effect of food, or the energy needed for digestion, absorption, and the metabolization or storage of nutrients; and the energy required for exercise or non-exercise activity<sup>46</sup>. Despite the relatively simple underlying mechanism of energy balance, in free living conditions some individuals are more prone to weight gain while others appear more resistant to weight changes<sup>47</sup>. Body size and composition are associated with one's resting metabolic rate, where larger body sizes generally have greater FFM, which possess higher degrees of metabolic activity and thus, higher resting metabolic rate. Similarly, the energy cost of PA increases with larger body size, though an inverse relationship exists between body size and PA levels<sup>48</sup>. When normalizing estimations of energy expenditure (EE) for body size and composition, EE appears to remain stable throughout the adult life until approximately 63 years of age, though large variance in EE between individuals still exist<sup>49</sup>.

Given the dual roles of energy intake and PA on energy balance, the simple suggestion to “eat less and move more” has become a commonly used heuristic to

promote weight loss, but neglects the complexity of the individual responses to exercise, diet, and personal environment (social, geographical), and socioeconomic status. For individuals with overweight or obesity, the ACSM recommends restricting energy intake to achieve 5-10% weight reduction within one year<sup>50</sup> and increasing PA to meet or exceed the minimum ACSM guidelines of 30 min of moderate-intensity PA five times each week or 20 min of vigorous-intensity activity for three days each week to minimize health risks<sup>51</sup>. Despite the seemingly simplistic concept of energy balance, weight management proves far more complicated in practice. For example, EE appears to plateau with increasing PA levels. Pontzer et al. observed that individuals in the 60<sup>th</sup> to 100<sup>th</sup> percentiles of PA saw a plateau in additional EE that was statistically indistinguishable from zero<sup>52</sup>, suggesting that additional PA is not strictly additive in terms of EE. Further, success rates for sustaining body weight following weight loss interventions are exceedingly low, with only around 20% of individual's from the general population reporting successful 1-year follow-up weight loss maintenance<sup>53</sup>.

Individual differences in response to diet and exercise, as well as an individual's environment and SES, add to the difficulty in addressing the prevalence of obesity. For instance, reductions in body weight induce concomitant decreases in EE. One study investigating individuals with obesity indicated that caloric restriction of 25% resulted in a lower TDEE at 6 months compared to baseline<sup>54</sup>. When accounting for how the changes in FM and FFM affect TDEE, the caloric restriction intervention accounted for a change in TDEE of  $-209 \pm 114$  kcal/day at six weeks and caloric restriction plus exercise accounted for  $129 \pm 86$  kcal/day at six weeks<sup>54</sup>, which has been observed elsewhere<sup>55</sup>. Regarding income and obesity, it has been observed that individuals with low-income

were more likely to develop obesity and those with obesity were more likely to have lower wages<sup>56</sup> and education<sup>57</sup>. Racial disparities in obesity prevalence exist, where non-Hispanic Asian adults represent the lowest rates at 17.4% while non-Hispanic Black/African-American adults represent the highest rates at 49.6% followed by Hispanic (44.8%) and non-Hispanic white adults (42.2%)<sup>4</sup>. Benusic and Cheskin (2021) note that when income is controlled, there is no greater risk of obesity among Black or Hispanic populations when compared to White populations<sup>57</sup>. The complex interplay of variables that coincide with high incidences of obesity are important to understand as the comorbidities of obesity threaten the health of at-risk populations.

The diagnosis of obesity is subject to many challenges, current evidence suggests that anywhere from 65% to 89.8% of individuals go undiagnosed<sup>58-60</sup> despite 39% of adults having overweight or obesity, globally<sup>61</sup>. This does not account for the individuals in the US that go without a source of primary care, a number that is growing, as from 2002-2015 there were significant reductions in reported primary care receipt for all age groups except for those in their 80s, with the largest decreases in younger age groups<sup>62</sup>. Given the relationships between obesity and T2D, hypertension, dyslipidemia, and CVD, a diagnosis of obesity is often the initial step in the treatment or prevention of these comorbidities. For individuals with obesity there is often an increased accumulation of lipids in the muscle and liver, increasing the risk of T2D<sup>63,64</sup> which is characterized by insulin resistance. In a sample of individuals with overweight and obesity, Calanna observed that those with prediabetes and T2D had higher basal insulin levels than the control group and significantly higher prevalence of liver steatosis in prediabetic and T2D patients<sup>65</sup> indicating excessive hepatic lipid storage. 4-hydroxynonenal, a biomarker

produced by the peroxidation of lipids, was observed by Ingram et al. to be significantly higher in insulin resistant individuals compared to those who were insulin sensitive, indicating the presence of elevated intramyocellular lipids in individuals with T2D<sup>66</sup>.

The presence of T2D greatly raises the risk of developing severe complications. Without management, T2D can increase an individual's risk of microvascular complications which could lead to the development of diabetic neuropathy, peripheral neuropathy, and diabetic retinopathy<sup>67</sup>. Diabetic neuropathy affects the peripheral nervous system, causing neurodegeneration starting with sensory axons, autonomic axons, and motor axons<sup>68</sup>. Peripheral neuropathy has a high prevalence rate, effecting 28% of diabetic hospital patients, and in a literature review by Ziegler et al., it is noted that among individuals with idiopathic peripheral neuropathy, 35% to 62% of patients are reported to have prediabetes<sup>69</sup>. Diabetic retinopathy, a highly prevalent condition<sup>70</sup> that causes damage to blood vessels of the retina, can potentially lead to vision impairment and blindness<sup>71</sup>. In T2D, damage to nerves caused by peripheral neuropathy can result in numbness or tingling in the feet leading to the reduced ability to sense pain and potential biomechanical abnormalities which, when in combination with repetitive external or minor trauma, can result in the development of foot ulcers<sup>72</sup>. It is predicted that between 15-34% of persons with diabetes will be effected at some point by diabetic foot ulcers<sup>72</sup>. A major complicating factor with the occurrence of foot ulcers is concomitant circulation issues that lead to slow wound healing, which in combination with sensory deficiencies may lead to unnoticed infections and eventually amputation. In a study by Prompers et al. examining a cohort of 1,088 diabetic foot ulcer patients, it was observed that 23% of



patients had not healed with peripheral neuropathy and peripheral artery disease being noted as predictive of non-healing<sup>73</sup>.

The consumption of highly processed food may be a causal factor in the development of a positive energy balance and subsequent weight gain. In a randomized controlled trial by Hall et al., 10 male and 10 female weight stable adults were admitted to a metabolic ward for 28 days where three daily energy and macronutrient matched meals were provided for ad libitum consumption<sup>74</sup>. During consumption of an ultra-processed diet, energy consumption, carbohydrate and fat, and sodium intake were greater during the ultra-processed diet compared to the unprocessed diet<sup>74</sup>. In a cohort study on weight gain and BP, Sundström et al. observed that for each 10 kg weight gain between 20 years and mid-life there was a 2.2 mmHg and 1.7 mmHg systolic and 3.2 mmHg and 2.4 mmHg diastolic increase in BP for men and women, respectively<sup>75</sup>. The excessive sodium consumption with ultra-processed may account for increases in BP associated with weight gain<sup>76,77</sup>. A lack of PA may also explain, in part, the increased BP with weight gain. There is a large body of literature exploring the role of PA in the prevention of hypertension, which indicates that individuals who regularly participate in PA (minimally meeting the ACSM recommendations) are at lower risk for developing hypertension<sup>78,79</sup>. In fact, among US adults the prevalence of low-HDL cholesterol from 2011-2014 was highest in individuals who failed to meet PA guidelines (21%) compared to those who did (17.7%)<sup>80</sup>.

Among preventable risk factors, high systolic BP is the leading cause of mortality worldwide and in 2017 accounted for 10.4 million deaths, globally<sup>81</sup>. Hypertension is a major concern in the presence of obesity and its relationship with obesity has been well

established in the literature<sup>82-84</sup>. The development of hypertension in obese individuals may be attributed to the excess accumulation of adipocytes leading to altered adipokine levels. In their review on the link between obesity and CVD, Nakamura et al. note that for individuals with obesity there is an upregulation in pro-inflammatory adipokine activity such as elevations in tumor necrosis factor- $\alpha$  and leptin as well as low levels of the anti-inflammatory adipokine, adiponectin<sup>85</sup>. In a study on 154 obese individuals, including 98 patients with some combination of hypertension, T2D, and dyslipidemia, Csongrádi et al. observed that adipokines were closely related to intima-media thickness which in turn had significant positive relationships with markers of hypercoagulation and impaired fibrinolysis, suggesting adipokine levels in obesity play a role in the development of atherosclerosis<sup>86</sup>.

Atherogenesis appears to be triggered by a combination of the above mentioned obesity related changes in adipokine activity and increases in pro-inflammatory cytokines from excess adiposity as well as changes in vasoconstrictor hormones and increased expression of adhesion molecules that promote clotting in the inner surfaces of the arterial wall<sup>87,88</sup>. Impaired nitric oxide release may also be implicated with altered adipokine activity, leading to endothelial vasoconstriction, and dysfunction<sup>89</sup>. An increase in endothelial permeability allows low-density lipoproteins (LDL) to bind to the subendothelial space where they are oxidized and signal a pro-inflammatory protective mechanism; further signaling macrophages which become foam cells as they attack, consume, and become saturated with oxidized LDL<sup>90,91</sup>. If foam cells fail to remove the LDL, as in the presence of chronic elevated levels of LDL, apoptosis will occur causing the release of the macrophage's lipid contents, promoting a cycle of increasing foam cell

accumulation<sup>90</sup>. Replication of foam cells can result in the formation of lesions, also known as fatty streaks, which are the first visible indicator in the progression of atherosclerosis and precede the formation of larger plaque structures<sup>90,92,93</sup>. More complex plaque structures are formed as the foam cells release cytokines and growth factors that stimulate vascular smooth muscle cell growth within the intima, forming a fibrous capsule over the fatty streak<sup>94,95</sup>. Yet, as macrophages continue to attack apoptotic cells within the extracellular matrix, they promote matrix-degrading enzymes, such as metalloproteinase, which break down the fibrous cap and structural scaffold of the plaque, making it vulnerable to rupture<sup>94,96</sup>.

A large body of research exists that links the presence of obesity and its atherogenic effects to an increased risk for developing a wide range of comorbidities. In a review on obesity disease risk, Gadde et al. reported that increases in BMI are associated with higher risk of heart failure, atrial fibrillation, CVD, hypertension, and left ventricular hypertrophy<sup>97</sup>. The presence of chronic hypertension, atherosclerosis, and stenosis ultimately result in increased myocardial afterload which puts greater strain on the heart and can lead to hypertrophy of the left ventricle. According to the Framingham Heart Study, left ventricular hypertrophy is a strong independent predictor for both CVD and coronary artery disease (CAD)<sup>98</sup>. This is further supported by the LIFE study which found that patients with CAD had around 80% higher left ventricular mass and 20% greater left ventricular stress than those without<sup>99</sup>. Pathological left ventricular hypertrophy can decrease the contractility of the left ventricle resulting in reduced cardiac output and ability to meet the oxygen demands of the body, which can eventually lead to the symptoms of heart failure<sup>100</sup>. Additionally, occluded blood flow due to plaques in the

coronary arteries may prevent adequate oxygen delivery to the myocardium<sup>101</sup>. Heart failure can occur in both the left and right side, both of which can be caused by CAD, hypertension, and right-sided heart failure can also be caused by pulmonary valve stenosis and pulmonary embolism<sup>102</sup>.

Atherosclerotic regions contribute to the development of peripheral arterial disease<sup>103</sup>, and lesions that are vulnerable to rupture are the main factor contributing to the development of luminal thrombosis<sup>94</sup>. In their review on sudden cardiac death, Virmani et al. note the prevalence of thrombi in sudden coronary death range anywhere from 20-70% and in acute myocardial infarction between 70-80%<sup>104</sup>. Gongora-Rivera et al. examined the prevalence of coronary atherosclerosis in patients with fatal strokes and reported that 72% had plaque occlusions and 38% stenoses causing occlusion greater than 50%<sup>105</sup>. In a study on patients with pulmonary embolism, Keller et al. investigated the impact of symptomatic atherosclerosis, defined as the presence of concomitant CAD, myocardial infarction, ischemic stroke, peripheral arterial disease, and arterial atherosclerosis. Symptomatic atherosclerosis was associated with worse health outcomes than asymptomatic patients with pulmonary embolism, including increased in-hospital adverse events and death, independent of other risk factors<sup>106</sup>. Khan et al., in their review on venous thromboembolisms, report that among patients diagnosed with pulmonary embolism, the mortality rate is around 20% within 1 year of diagnosis<sup>107</sup>, and Konstantinides et al. report that long-term follow up studies indicate that as much as 50% of patients who have suffered an acute pulmonary embolism episode have persistent reductions in quality of life<sup>108</sup>. The development of vascular diseases associated with

adiposity pose a serious health risk, with the contributing factors being descriptive of the clustering of risk factors associated with MetS.

As previously discussed, MetS is a clustering of abdominal obesity, dyslipidemia, hypertension, and elevated FBG. The prevalence of MetS remains high in the US with a reported incidence of 23-34.7% from 2014-2016<sup>12,109,110</sup> with rates being lowest among adolescents and highest among those over 60 years of age<sup>4</sup>. Of particular concern, however, is the increased incidence from 16.2% in 2011-2012 to 21.3% in 2015-2016 in those aged 20 to 39 years<sup>12</sup>. Obesity rates have continued to rise in the among US, increasing from 33.7-39.6% and 16.8-17.2% from 2007-2008 to 2015-2016<sup>111</sup>, and up to 42.4% for 2017-2018<sup>4</sup>. While the incidence of obesity and diabetes continues to rise in the US, the overall incidence of MetS has not followed a similar trajectory<sup>12,109</sup>. Given that the prevalence in obesity and MetS are misaligned despite their well-established associations, appropriate screening is critical.

Screening of MetS risk requires assessment of each of the individuals risk factors, some of which are performed as part of regular physician visits, and others requiring more invasive testing. For assessments of fasting HDL, TG, and FBG, blood samples are drawn and analyzed for lipid and glucose levels. Blood glucose is traditionally measured with blood gas analyzers (BGAs), modern handheld BGAs, or cassette-based BGAs, which can produce accurate measurements of FBG<sup>112</sup>. Fasting venous blood samples can be drawn and analyzed for TG levels, LDL, HDL, and remnant cholesterol, which is composed of TG rich lipoproteins, very low-density lipoproteins, and intermediate-density lipoproteins, and are quickly degraded<sup>113</sup>. Cassette based blood analysis can also

provide fast readings of total cholesterol, HDL, LDL, total-to-HDL ratio, and very-low-density lipoprotein with overall correlation coefficients as high as 0.97<sup>114</sup>.

Another MetS factor is BP, which is measured by inflating the cuff of a sphygmomanometer to occlude blood flow of the brachial artery of the upper arm and auscultating the brachial artery. With a stethoscope the observer can listen for the return of the pulse as air is slowly released and the cuff relaxes. The pressure at which the first sound of a pulse is heard, also known as the first Korotkoff sound, indicates the systolic BP, and the pressure at which final audible sound is heard corresponds to the diastolic BP. As discussed earlier, untreated hypertension can lead to the development of a wide range of comorbidities. In a large systematic review by Bundy et al., a linear relationship between systolic BP level and CVD, stroke, and coronary disease was observed, and the lowest risk for CVD and all-cause mortality exists amongst those with systolic BP around 120-124 mmHg<sup>115</sup>. While bloodwork is needed for MetS screening, not all assessments are invasive.

WC is a non-invasive test performed with a tape measure, usually landmarked at either the superior border of the iliac crest or midway between the lowest ribs and the iliac crest. There is currently no standardization for WC measurement landmarking despite evidence suggesting that the anatomical location of the measurement may contribute to considerable differences in health risks<sup>116</sup>. Some evidence suggests that midway between the lowest ribs and iliac crest provides the best measurement for central obesity<sup>117</sup>. WC provides a predictive measure for excess abdominal adiposity, and while not part of MetS screening, HC, and WHR may further help predict the risk of abdominal obesity. Abe et al. demonstrated a significant positive association with both BMI and WC

in prediction of diabetes<sup>118</sup>. Gadekar et al. observed very strong correlations between WHR and VAT as assessed by MFBI, and moderate and strong correlations between VAT and WC for males and females, respectively<sup>20</sup>. Measures of WC and HC additionally allow some differentiation between upper and lower body adiposity, an important distinction with multiple large population studies demonstrating increased risk of metabolic complications with increasing WC and HC with having an inverse relationship<sup>119,120</sup>. Cameron et al. observed when accounting for both WC and HC, specifically in individuals with smaller waists who would not normally be identified as high risk, the number of individuals classified with a high mortality risk increased by 19% and 18% for men and women, respectively<sup>20</sup>. In a review on the role of visceral adipose tissue and MetS, Wajchenberg notes that when compared to excess peripheral fat, central VAT is associated with higher incidence of insulin resistance, hyperlipidemia, and decreased HDL, independent of overall obesity<sup>8</sup>. Another review on the pathophysiology of visceral obesity by Tchernof and Després (2013) affirms the independent relationship between visceral adiposity and insulin resistance, as well as increased risk of atherosclerosis and thrombosis<sup>23</sup>. Given the pathogenic role of excess adiposity and adiposity distribution, more direct assessments of body composition may be warranted to better screen for disease risk.

## **2.2 Body Composition**

Many different techniques exist for body composition estimation. While many are well validated, they are limited by expense and access, or are prone to error by procedure assumptions, proprietary equations, pre-assessment standardization, and technician competency. Both MRI and CT are considered the most accurate body composition

assessments for total, visceral, subcutaneous, and interstitial adiposity, as well as provide detailed segmental analysis of skeletal muscle<sup>121</sup>. The technology is a continuation from an older nuclear magnetic resonance technology which relied on the unique magnetic properties of atomic nuclei, specifically hydrogen, which exists in large enough quantities and with a sufficiently large nucleus to permit the production of images via the mapping of measured magnetic field gradients<sup>122</sup>. In 1975, Paul C. Lauterber demonstrated that nuclear magnetic resonance could produce spatial information that generated multi-dimensional images, paving the way for the modern MRI now used for detailed medical imaging<sup>123</sup>. In fact, MRI is equipped to determine the quantity and location of abdominal adipose tissue, specifically the more pathogenic visceral adipose tissue (VAT), which is highly associated with MetS<sup>124</sup>. While full body scans can be completed in as little as 10 minutes, the analysis of the MRI image requires manual segmentation of the muscle can take up to several days<sup>125</sup> in addition to the cost of assessment.

CT is another method available for medical imaging. Instead of magnetic fields, CT utilizes X-rays that are rotated around a subject and projected through the plane of the area to be imaged. The technology was piloted in 1967 by Godfrey Hounsfield who first proposed X-ray beams could be directed through the body and through the attenuation of photons, producing cross-sectional images of the interior of the body<sup>126</sup>. The attenuation of X-ray beams provides information on the electron density distribution of the scanned areas<sup>121,127</sup>. Each X-ray beam yields a single pixel of information on tissue density, thus CT scans require a computer to convert the collected scan data into reconstructed detailed images of the scanned area<sup>128</sup>. Given the emission of X-rays in CT, there is exposure to a substantial dose of radiation, with a single abdominal scan exposing a patient to 3100



$\mu\text{Sv}$  compared to  $0.96 \mu\text{Sv}$  from a full body DXA scan<sup>129</sup>. Because X-rays emitted by CT are considerably greater than that of a conventional X-ray<sup>130</sup>, the risk may outweigh the benefit and limit the ability to perform routine assessments.

DXA provides a strong alternative to both MRI and CT by quickly providing full body scans and exposing the subject to substantially lower radiation. In 1963, Cameron and Sorenson (1963) first demonstrated that by utilizing low-energy photon beams, bone mineral content (BMC) could be measured<sup>131</sup>. By 1981 the technology evolved into dual photon absorptiometry, which was first demonstrated by Mazess et al. to be suitable for total bone mineral density by scanning dry skeletons, and further showed reliability when scanning the skeletons along with materials to proxy soft tissue<sup>132</sup>. The clinical application of DXA is typically the diagnosis of osteoporosis through measurements of bone mineral density<sup>133</sup>. DXA utilizes dual X-ray beams passed through the subject at different frequencies, and like CT, assesses attenuation of photon energy which provides density information for each beam to differentiate between bone mineral, FM, and lean soft tissue<sup>134</sup>. DXA scans for VAT show high correlation to CT VAT assessments<sup>135</sup>, as well as high correlations of VAT measures when compared to MRI assessments<sup>136,137</sup>. DXA has demonstrated agreement with the 4-compartment model for BF% among adults<sup>138</sup>, children and adolescents<sup>139</sup>, producing estimates of BF% within 1% to 3% of multicomponent models<sup>140</sup>. Low coefficients of variation have been reported for DXA measures of FM, FFM, and BMC among athletic and active individuals<sup>141</sup>. Further, DXA has demonstrated the ability to produce accurate and reliable assessments of skeletal muscle in adults<sup>142</sup>, children, and late stage pubertal adolescents<sup>143</sup>. DXA measures of VAT have also been correlated with insulin resistance and low-HDL, diastolic BP,

decreased peak  $\text{VO}_2$ , and high TG levels, supporting the use of DXA derived VAT for screening MetS risk<sup>144,145</sup>. DXA is not without limitations, however, as proportional biases exist with DXA tending to underestimate the BF% of leaner individuals<sup>146</sup>. Factors such as body size, sex, age, and disease state have all been shown to be independent contributors to the biases observed during DXA body composition assessments<sup>147</sup>, warranting careful consideration when deciding whether DXA is appropriate to use in different clinical populations. While the overall cost of a DXA scan is lower than MRI and CT, with substantially lower radiation exposure than CT, DXA remains a clinical assessment tool that is not universally accessible and can cost \$125 or more out-of-pocket<sup>148</sup>.

Indirect measurements of body tissues may also be used to predict body composition based on differing densities of FM and FFM. Specifically, hydrostatic weighing (HW) and air displacement plethysmography (ADP) can be used to predict body composition based on the 2-compartment model, which separates the body into all fat and non-fat tissues. HW is based on Archimedes' principle, which states that when a body is submersed in water, the upward force of buoyancy is equal to the weight of the fluid displaced by the body. Among body tissues, adipose is the only body tissue with a density less than water thus, differences in body composition at a fixed body weight will experience specific degrees of buoyancy. Due to the indirect nature of body volume assessment, the model used for converting densitometry to body composition must assume that the density of FM and FFM are constant<sup>121</sup>, and the assumed densities may differ across various groups<sup>149</sup>. For HW, participants are required to fully submerge themselves into a tank of water and maximally exhale to eliminate as much air from the

lungs as possible<sup>134</sup>. With 2-compartment models such as hydrostatic weighing, FFM density is assumed as a constant despite individual variations due to total body water and BMC thus, failure to directly assess residual volume within the lungs can affect the assessment of body density and predicted BF%, resulting in significant differences BF% values<sup>150</sup>. Expiration of residual lung volume underwater may be uncomfortable, require practice, and vary within individuals following weight changes or as age increases<sup>150</sup>; requiring careful consideration when deciding whether or not to use HW.

ADP is a newer method that assesses BV and densitometry based on the amount of air displaced by a body within an environmentally controlled space. ADP relies on Boyle's Law which states that there is an inverse relationship between pressure and volume of a gas when that gas is at room temperature. The most common tool for ADP is a BOD POD, which can be performed with significantly reduced participant burden, requiring only that the participant wear minimal, form fitting clothing and a swim cap to secure loose hair which may affect measurement accuracy. Residual lung volume is accounted for by the BOD POD system by utilizing pulmonary plethysmography to measure functional residual capacity, and like HW, body weight and body volume can be used to calculate body density which can then be used to estimate body BF% utilizing the Siri<sup>151</sup> or Brozek<sup>152</sup> equations. ADP assessment takes significantly less time, is less invasive, and is easier to access compared to HW. Further, ADP has demonstrated good test-retest reliability for assessment of body volume, FFM, resting metabolic rate, and BF%<sup>153</sup>. While more accessible than other body composition assessments ADP still requires access to a specialized facility with access to a BOD POD, and ADP may also be subject to significant error if a participant has loose clothing<sup>154</sup> or excessive facial hair,

and while ADP underestimates BF% in obese individuals compared to DXA, it has shown to track changes in body composition similar to DXA<sup>145,155</sup>.

While laboratory measurements provide the most robust assessments of body composition, mobile field-based assessments can provide access that would not otherwise be possible. Popular among field assessments are BIA and BIS, devices which predict body composition by measuring the electrical resistance of body tissue and differing hydration levels within body tissues. BIS assesses the impedance within an electrical circuit, which in the human body consists of intracellular fluid, extracellular fluid, and cell membrane capacitance measured by resistance and reactance, and thus measures of said variables can be performed<sup>156</sup>. The raw data from BIS can provide information of phase angle, an important measure of the integrity of the cell membrane. Higher phase angle values are associated with improved physical function<sup>157</sup>, while lower values are have been associated with increased mortality following ICU admission<sup>158</sup>, poorer survival in cancer patients<sup>159</sup>, and malnutrition<sup>160</sup>. Preassessment standardization is important for bioelectrical measures, which can be influenced by hydration status and food intake. Standardization requires assessment take place with an 8 hr fast from food and water and in a state of euhydration, which is necessary for both BIS and BIA to produce the most accurate and reliable results.

BIA is similar to BIS, but prediction of body composition requires population specific equations to convert impedance measures to BF%. BIA devices can utilize either single frequency BIA, which sends a single 50 kHz, or multi-frequency BIA (MF BIA) which sends multiple currents across various frequencies. Single frequency BIA is limited by the 50 kHz frequency which cannot completely penetrate tissue<sup>161</sup> and has

shown poor agreement for VAT measurement compared to CT<sup>162</sup>. While MFBIAs have demonstrated some correlation to VAT compared to CT, it did not significantly correlate with metabolic disease markers<sup>163</sup>. Relative to DXA, MFBIAs have shown a significant correlation with BF% and significant correlations with whole-body FFM<sup>164</sup> and segmental FFM, but consistently underestimate both FM and BF% while overestimating FFM<sup>165</sup>. Given the strong correlations, and despite absolute differences, MFBIAs show no significant difference to DXA when tracking changes in FM, FFM, and BF% over time<sup>166,167</sup>. BIS and BIA can provide valuable tools for tracking changes in body composition, but the highest quality devices can be expensive and not widely accessible. Further burden may be introduced by the need to standardize measurements for the most reliable assessments which requires subjects to refrain from consumption of food or liquids, and alcohol, caffeine, or other diuretics, and refrain from exercising for at least 8 hours prior to assessment<sup>168</sup>.

Among the most widely accessible body composition assessment techniques are skinfold (SKF) measurements. The only tool required for SKF assessment is a SKF caliper, which measures the thickness of SKF from various body sites, and through specific equations can predict body density and composition. The most commonly used equations were developed by Jackson and Pollock for both men<sup>169</sup> and women<sup>170</sup>. These equations utilize seven SKF sites, taken at the chest, triceps, axilla, subscapular, abdominal, suprailiac, and thigh<sup>169</sup>. While BF% calculated from SKF agree with DXA derived BF%, SKF tends to underestimate BF% in both obese and non-obese females<sup>171</sup>, and biases are found with SKF BF% across ethnic groups<sup>172</sup>. There exists a wide array of available equations that use as little as two or as many as seven skinfold sites, with 2-, 3-,

and 7-site equations having demonstrated agreement with DXA BF%<sup>173</sup>. SKF equations are limited by their reliance on a 2-compartment model, though 4-compartment validated equations may help improve accuracy<sup>174,175</sup>. As a simple measurement, SKF is a desirable field measure, but its validity is dependent on utilizing the correct equations, and its reliability dependent on the observer's skill and ability to produce consistent measurements<sup>176</sup>.

### **2.3 Smartphone 3D Body Scanning Applications**

With the computational power of a personal computer, the capabilities of the modern smartphone have far surpassed simple communication. Utilizing the built in camera and microphone, smartphones and smartphone-connected wearables can capture cardiovascular activity data such as heart rate and heart rate variability, eye health, respiratory and lung health, and skin health<sup>177</sup>. The presence of motion sensors such as accelerometers, gyroscopes, proximity sensors, and global positioning systems allows for the collection of measures such as daily activity, fall tracking, and sleep monitoring<sup>177</sup>. Given the prevalence of obesity and metabolic disease, many health and fitness applications focus on providing tools to support weight loss. In a retrospective cohort study by Chin et al., the data from 35,921 users of a popular weight loss app collected across 76 weeks showed 77.9% of users reported a decrease in body weight while using the app<sup>178</sup>. A recent randomized controlled trial by Cho et al. looked at the effectiveness of smartphone-based lifestyle coaching, finding that application use supported BF% reduction although it did not yield changes in systolic BP<sup>178</sup>. Despite such positive potential, the overabundance of commercially available apps may result in varying levels of effectiveness, which necessitates caution when seeking weight loss support from this

technology<sup>179</sup>. While the body of literature investigating the efficacy of mobile application interventions for weight loss continues to grow<sup>180</sup>, there is little current research exploring the use of smartphone technology for assessing or screening for metabolic health risk.

Recently, body scanning, which utilizes either 2- or 3-dimensional imaging, has shown promise as a quick and non-invasive alternative to traditional body composition assessments. The proprietary nature of the 3DO scanning technology presents a major limitation, but it is a limitation shared by nearly all body composition prediction methods. While 3DO scanning is still a relatively new technology for anthropometric assessments, the burgeoning research continues to indicate that the technology has promise as an alternative assessment tool for body composition. Tinsley et al. have demonstrated strong equivalence between body composition measurements from commercially available 3DO scanners ( $\pm 1.3\%$  BF%,  $\pm 1.0$  kg FM,  $\pm 2.7$  kg FFM)<sup>35</sup> and 4-compartment model estimates. Further, 3DO scanning has produced fat mass index (FMI) values comparable to both BIA and skinfold assessments as well as VAT measurements comparable to DXA<sup>36</sup>. 3DO scanning has also demonstrated strong associations in adolescents when compared to DXA measures of BF%, FM, FFM, and VAT<sup>181</sup>. Tian et al. demonstrated that two dimensional photographs taken with a consumer level digital single-lens reflex camera can successfully predict 3D body shape and from that, body composition<sup>182</sup>. While the body of literature supporting the efficacy of 3DO scanning for body composition continues to grow, newer research has begun to validate its use for more anthropometric measures and health risk screening.

In comparison to standard tape circumference measures, 3DO scanning has demonstrated strong associations for WC and HC measures and body surface area (BSA)<sup>181</sup>. To account for software differences between devices, Sobhiyeh et al. developed a “universal” software for standardizing anthropometric body dimensions gathered from different devices<sup>34</sup>. Measurements of WC and HC from the three commercially available 3DO devices used were highly correlated ( $R^2$ : 0.95 – 0.97) when compared to conventional tape measure assessments<sup>34</sup>. In an analysis examining the test-retest reliability of four commercially available 3DO scanners utilizing each device’s prepackaged software, Tinsley et al. observed high precision for all device’s individual circumference measures and high precision between the averages of all body regions measured by each device<sup>183</sup> suggesting manufacturer software reliability. Bourgeois et al. have also demonstrated significant correlations between 3DO circumference measurements and flexible tape measures ( $R^2$ : 0.71 – 0.96) for three 3DO systems with proprietary image processing software<sup>184</sup>. Despite the aforementioned benefits of 3DO scanning, the technology is expensive and limited to research and fitness/ health club settings.

The high-quality cameras found on modern smartphones may provide an opportunity to make important health metrics from 3DO scanning broadly accessible. Preliminary findings on M-3DO via smartphones indicate that M-3DO circumference measurements agree with conventional tape measurements<sup>185,186</sup>. In assessing the validity of a commercially available M-3DO application, Neufeld et al. observed acceptable validity in WHR measurements compared to tape measurements, despite poor agreement on absolute measures, and agreement with both BIA and SKF<sup>187</sup>. BF% produced from



two two-dimensional images taken on a smartphone camera and processed using a trained convolutional neural network has shown to be highly associated with BF% produced by DXA for both males and females; even outperforming BIA and ADP<sup>37,186</sup>. Much of the findings on mobile body scanning are preliminary, but the technology may have the potential to provide access to high quality anthropometric evaluations to every smartphone owner, bridging the gap between physician and patient. While 3DO scanning has shown correlation with biomarkers of MetS<sup>36</sup>, there is currently no literature investigating such relationships with M-3DO. Thus, the purpose of this thesis is to determine the predictive ability of a validated M-3DO application for determining metabolic health risks in adults.

## CHAPTER III - Methods

### 3.1 Participants

For this cross-sectional study, we prospectively recruited 62 participants, between the ages of 18 and 75 years ( $29.52 \pm 11.21$ ). Participants were excluded if they were younger than 18 or older than 75, were missing any limbs or part of a limb that may influence assessment accuracy; had any injury or mobility limitation that would prevent participation; were pregnant; breast feeding; or lactating. The study began in November 2022 and continued until March 2023. Further, the study was conducted according to the guidelines set forth by the Declaration of Helsinki and all procedures involving human participants were approved by the University of Southern Mississippi ethics committee (IRB #22-1012). Written and informed consent was obtained prior to participation.

Participants were recruited by word of mouth and through digital advertisements posted/sent around the USM campus and through USM newsletters, newspapers, and social media platforms, and announcements made in classrooms or virtual classrooms of faculty or staff in the School of Kinesiology & Nutrition at the University of Southern Mississippi, as well as surrounding communities such as medical clinics and churches. Prior to posting advertisements, permission was obtained from medical clinics, churches, or any additional community entity. To prevent the possibility of undue influence or coercion, potential participants were informed that participation was completely voluntary and that they were able to withdraw at any time without penalty.

### 3.2 Procedures

Participants reported to the laboratory following  $\geq 8$  h of abstention from food, beverages, supplements and medications, and abstention from exercise for  $\geq 24$  h.

Adherence to pre-participation protocols were confirmed by an investigator during pre-assessment screening. Upon completion of pre-assessment screening, participants were instructed to remove externally worn metal and all other accessories, and complete body composition and anthropometric assessments in the following sequence: body mass, height, body circumferences, traditional booth 3DO scanning, and smartphone 3DO application. After a minimum of five minutes in a seated position with feet flat on the floor, resting BP was assessed using a digital BP monitor (HEM-907XL, Kyoto, Japan). Following BP assessments, height was collected using a stadiometer (SECA 769, Hamburg, Germany) and weight using a calibrated digital scale (SECA, Hamburg, Germany). WC was collected using a standard spring-loaded aluminum tape measure, wrapped around the torso horizontally with minimal tension to avoid compression of the skin and subcutaneous adipose layer. The tape measure was placed in the horizontal plane around the abdomen at the level of the uppermost level of superior iliac crest<sup>188</sup>. Following anthropometric and 3DO scans, fasting blood lipids and FBG were assessed using a point-of-care cholesterol analyzer (Cholestech LDX Analyzer, Abbot<sup>®</sup>, Abbott Park, IL).

### **3.3 Mobile 3-Dimensional Imaging Analysis**

Body composition estimates from traditional 3DO scanning were performed using the Mobile+Fit Booth (Size Stream LLC, Cary, NC, USA) (3DO<sub>Booth</sub>) and smartphone estimates was performed using the MeThreeSixty<sup>®</sup> application (Size Stream LLC, Cary, NC) on an iPhone 12 Pro<sup>®</sup> (Apple Inc., Cupertino, CA, USA) (3DO<sub>App</sub>) (MeThreeSixty<sup>®</sup>, Size Stream LLC, Cary, NC, USA). Both the 3DO<sub>Booth</sub> and 3DO<sub>App</sub> have been reported to produce acceptable reliability for anthropometric measurements when compared to a

reference tape measure<sup>185</sup>. For both the 3DO<sub>Booth</sub> and 3DO<sub>App</sub>, participants were instructed to wear tight fitting clothing, remove any external accessories, and tie long hair up so that none fall below the shoulders. The 3DO-T encloses the participant in a booth comprised of three walls and a curtain used for entry, with the participant instructed to stand at the end of the booth opposite the 3DO scanner. The participant was instructed to enter the booth, and the curtain was closed prior to beginning the scan to ensure consistent lighting.

Procedures for 3DO-SM have been described elsewhere<sup>189,190</sup> but are summarized below. The phone was placed on a fixed tripod at an approximated average waist height (91.0 cm) for all participants and the participants were set up to stand at a distance deemed acceptable by the application. Each assessment consisted of two images where 1) the participant was facing the camera with arms and feet positioned away from the torso to a position deemed acceptable by the manufacturer and 2) the participant was turned to their left side so that their right shoulder was facing the camera and standing with hands and feet together and aligned so that they were within the silhouette of the trunk.

### **3.4 Metabolic Health Assessment**

The metabolic health markers LDL, HDL, TG, and FBG were assessed by fingerstick using a capillary blood analyzer. The analyzer was calibrated each day prior to testing and multi-analyte controls were conducted based on the manufacturer recommendations. Following standard sanitation and preparatory procedures, 40  $\mu$ L of blood were collected from the fingertip into heparin-lithium lined capillary blood tubes and placed into individual cassettes (Cholestech LDX Lipid Profile•GLU, Abbot<sup>®</sup>, San Jose, CA, USA) for analysis. TG measurements > 650 mg/dL are not recorded using this

device, and measurements of HDL are not recorded for TG > 650 mg/dL. Thus, participants with TG > 650 mg/dL (n = 2) had their TG recorded as 650 and their HDL recorded as the average of sex, race/ethnicity, and MetS classification matched adults. BP was measured using a manual sphygmomanometer and BP cuff after the participant had been seated for  $\geq 5$  min with their feet flat on the floor. For the assessment, the BP cuff was placed around the arm to occlude the brachial artery upon inflation. The cuff was manually inflated to  $\simeq 20$  mmHg above systolic BP. Elevated BP was defined as systolic between 120 and 129 mmHg and diastolic  $\leq 80$  mmHg, and hypertension was defined as systolic  $\geq 130$  mmHg and diastolic  $\geq 80$  mmHg<sup>191</sup>.

### 3.5 Metabolic Health Risk Score

Calculation of MetS severity (MSs) were conducted using sex and race/ethnicity specific MetS risk score equations produced by Gurka<sup>192</sup> (2-5):

$$(1) \text{ Male Non Hispanic White} = -5.4559 + 0.0125(WC) - 0.0251(HDL) + 0.0047(SBP) + 0.08244(\ln(Tri)) + 0.0105(Glu)$$

$$(2) \text{ Male Non Hispanic Black} = -6.3767 + 0.0232(WC) - 0.0175(HDL) + 0.0040(SBP) + 0.5400(\ln(Tri)) + 0.0203(Glu)$$

$$(3) \text{ Male Hispanic} = -5.5541 + 0.0135(WC) - 0.0278(HDL) + 0.0054(SBP) + 0.8340(\ln(Tri)) + 0.0105(Glu)$$

$$(4) \text{ Female Non Hispanic White} = -7.2591 + 0.0254(WC) - 0.0120(HDL) + 0.0075(SBP) + 0.5800(\ln(Tri)) + 0.0203(Glu)$$

$$(5) \text{ Female Non Hispanic Black} = -7.1913 + 0.0304(WC) - 0.0095(HDL) + 0.0054(SBP) + 0.4455(\ln(Tri)) + 0.0225(Glu)$$

$$(6) \textit{Female Hispanic} = -7.7641 + 0.0162(WC) - 0.0157(HDL) + 0.0084(SBP) + 0.8872(\ln(Tri)) + 0.0206(Glu)$$

### 3.6 Prediction Modelling

Body Composition and anthropometric variables were extracted from each 3DO scanning technique to determine their ability to predict MetS. Variables produced from each 3DO scanning technique were included into the omnibus regression model predicting MSs. Backwards stepwise regression was used to produce a final model.

### 3.7 Statistical Analyses

Precision error (PE), root mean square coefficients of determination (RMS-CV%), and two-way, random effects, absolute agreement intraclass correlation coefficients (ICC) were used to determine the test-retest reliability and precision between body composition and body circumference metrics produced by the 3DO<sub>Booth</sub> and 3DO<sub>App</sub>; each of which employ the same algorithms to produce these estimates.

Following determination of acceptable inter-device precision, body composition estimates produced by the 3DO<sub>App</sub> were entered as predictor variables for MetS in linear regression models which included: BF%, FM, FFM, and BSA; WC, stomach (SC), hip, shoulder width (SW), chest (ChC), upper arm (AC), forearm (FC), thigh (TC), and calf (CC); and common body composition indices produced by the 3DO model including fat mass index (FMI), fat-free mass index (FFMI), WHR, and waist-to-height ratio (WHt). FMI and FFMI were calculated as the tissue in question (in kgs) divided by height (in meters) squared. WHR was calculated as the WC divided by the HC and WHt was calculated as WC divided by height (in cm). Because the device produces individual appendicular circumference estimates, all appendicular circumference (i.e., estimates

pertaining to the arms and legs) predictor variables were averages of the left and right sides. To account for the influence of stature, height, weight, and BMI were also included as predictor variables.

To develop prediction equations for MSs, backwards linear regressions were conducted for the total sample, and males and females independently across three separate models. The “body composition” model included BF%, FM, FFM, FMI, FFMI, and BSA. The “anthropometric” model included height, weight, BMI, WC, SC, HC, SW, ChC, AC, FC, TC, and CC. The “combined” model included all measures from the preceding models. Final models were determined as those producing the highest adjusted  $R^2$  and lowest mean square error (MSE).

Following the creation of each individual model, the performance of each model in predicting MetS-S was assessed using paired t-tests, Pearson correlations ( $r$ ), coefficients of determination ( $R^2$ ), and individual error was assessed using root mean square error and Bland-Altman analyses. Mean differences were defined as the predicted MSs minus the actual MSs. Statistical significance was determined at  $p < 0.05$  and all data was analyzed using IBM SPSS version 27 and Microsoft Excel version 16.

CHAPTER IV - RESULTS

**4.1 Participants**

Participant characteristics are demonstrated in Table 4.1. Among participants with less than three MetS risk factors, 48.4% (n = 30) had at least one risk factor. In addition, 33% were classified as having obesity.

**Table 4.1** Physical characteristics of study participants

		<b>Total</b>	<b>Male</b>	<b>Female</b>
<b>Sex</b>		62 (100%)	26 (42%)	36 (58%)
<b>Anthropometry</b>	Age (years)	29.52 ± 11.21	28.96 ± 9.46	29.92 ± 12.44
	Height (cm)	168.29 ± 10.41	177.21 ± 8.19	161.84 ± 6.25
	Weight (kg)	79.89 ± 22.65	93.92 ± 21.03	69.76 ± 18.07
	BMI (kg/m <sup>2</sup> )	27.93 ± 6.42	29.85 ± 6.43	26.55 ± 6.13
	Body Fat (%)*	28.98 ± 7.62	24.17 ± 7.56	32.45 ± 5.54
	FM (kg)*	23.69 ± 11.18	24.00 ± 12.31	23.46 ± 10.47
	FFM (kg)*	80.04 ± 22.70	94.10 ± 21.06	69.88 ± 18.11
	Waist (cm)	89.36 ± 16.16	96.85 ± 15.56	83.95 ± 14.51
	Hip (cm)	105.51 ± 11.32	107.68 ± 10.57	104.94 ± 11.73
	WHR	0.87 ± 0.07	0.90 ± 0.07	0.85 ± 0.07
<b>Race</b>	White	44 (71%)	16 (62%)	28 (78%)
	Black/AA	16 (26%)	10 (38%)	6 (17%)
	Asian	2 (3%)	0 (0%)	2 (5%)
<b>Ethnicity</b>	Hispanic	8 (13%)	3 (12%)	5 (14%)
<b>BMI Classification</b>	Normal Weight (< 25 kg/m <sup>2</sup> )	19 (31%)	4 (15%)	15 (42%)
	Overweight (25 - 30 kg/m <sup>2</sup> )	23 (37%)	10 (38%)	13 (36%)
	Class I Obesity (30 - 35 kg/m <sup>2</sup> )	11 (18%)	8 (31%)	3 (8%)
	Class II or Higher Obesity (> 35 kg/m <sup>2</sup> )	9 (15%)	4 (15%)	5 (14%)

Note: BMI, body mass index; AA, African American; FM, fat mass; FFM, fat-free mass; WHR, waist-to-hip ratio.

Data are presented as n (% of the column total)

\*Estimates produced by 3DO-SM



## 4.2 Precision Analyses

Results of the precision analysis are reported in Table 2. ICC for all variables ranged from 0.881 to 0.991 (all  $p < 0.001$ ), indicating adequate test-retest reliability between devices (smartphone and tablet-based applications). PE ranged from 0.00 to 2.56 for all anthropometric variables and 0.41 to 1.25 across all body composition variables, and 61.4 for BSA. FM and FMI had the highest root mean square coefficient of variation for all variables (4.59 and 4.35, respectively).

## 4.3 Body Composition Models

For the total sample, the final model included the variables BF% and FFMI which produced an  $R^2$  of 0.49 ( $r: 0.70$ , MSE: 0.34,  $p = 0.001$ ). For the females only sample, the final model included BF% and had an  $R^2$  of 0.52 ( $r: 0.72$ , MSE: 0.253,  $p < 0.001$ ). For the males only sample, the final model included FMI (Table 4.2) and had an  $R^2$  of 0.43 ( $r: 0.66$ , MSE: 0.476,  $p < 0.001$ ).

**Table 4.2** Body composition model summary

	$\beta$ (95%CI)	$r$ ( $R^2$ )	p-value
Total			
BF%	0.043 (0.023, 0.063)	0.47 (0.22)	< 0.001
FFMI	0.120 (0.077, 0.163)	0.57 (0.32)	< 0.001
Females			
BF%	0.093 (0.093, 0.124)	0.72 (0.52)	< 0.001
Males			
FMI	0.148 (0.077, 0.22)	0.66 (0.43)	< 0.001

Note: BF%, body fat percentage; FFMI, fat free mass index; FMI, fat mass index

## 4.4 Anthropometric Models

For the total sample, the final model included the anthropometric variables WHt, SC, HC, AC, FC, ChC, and SW and had an  $R^2$  of 0.60 ( $r: 0.77$ , MSE: 0.289,  $p < 0.001$ ). For the females only sample, the final model included the anthropometric variables WHt,

BMI, WC, and ChC and had an  $R^2$  of 0.64 (r: 0.80, MSE: 0.207,  $p < 0.001$ ). The final model for male participants included the anthropometric variables BMI, WC, SC, weight, AC, CC, and FC (Table 3) which produced an  $R^2$  of 0.65 (r: 0.81, MSE: 0.391,  $p = 0.003$ ).

**Table 4.3** Anthropometric model summary

	$\beta$ (95%CI)	r ( $R^2$ )	p-value
<b>Total</b>			
Wht	16.19 (8.04, 24.34)	0.72 (0.52)	< 0.001
Stomach	-0.07 (-0.14, -0.01)	0.68 (0.46)	0.027
Hip	0.05 (0.00, 0.10)	0.63 (0.40)	0.037
Biceps	-0.28 (-0.50, -0.06)	0.60 (0.36)	0.015
Forearm	0.47 (0.11, 0.83)	0.53 (0.28)	0.012
Chest	0.06 (-0.02, 0.13)	0.66 (0.44)	0.132
Shoulder	-0.72 (-1.44, 0.01)	0.56 (0.31)	0.052
<b>Females</b>			
Wht	13.27 (3.16, 23.37)	0.78 (0.61)	0.012
BMI	-0.09 (-0.12, 0.03)	0.68 (0.46)	0.197
Waist	-0.09 (-0.20, 0.03)	0.74 (0.55)	0.131
Chest	0.08 (-0.01, 0.17)	0.74 (0.55)	0.089
<b>Males</b>			
BMI	0.42 (0.17, 0.67)	0.67 (0.45)	0.003
Waist	-0.06 (-0.16, 0.04)	0.63 (0.40)	0.250
Stomach	0.02 (-0.07, 0.11)	0.62 (0.38)	0.673
Weight	-0.10 (-0.19, -0.01)	0.62 (0.38)	0.035
Biceps	-1.12 (-1.87, -0.36)	0.54 (0.29)	0.006
Calf	0.25 (-0.25, 0.75)	0.56 (0.31)	0.314
Forearm	1.72 (0.37, 3.08)	0.55 (0.30)	0.016

Note: Wht, waist-to-height ratio; BMI, body mass index

#### 4.5 Combined Models

For the total sample, the final model included the variables BF%, FM, FMI, FFMI, SW, ChC, AC, SC, HC, and Wht and had an  $R^2$  of 0.64 (r: 0.80, MSE: 0.270,  $p < 0.001$ ). For the females only sample, the final model included the variables BF%, FM, FMI, BSA, SW, ChC, FC, SC, and WHR and had an  $R^2$  of 0.77 (r: 0.88, MSE: 0.160,  $p < 0.001$ ). For the males only sample, the final model included the variables BF%, FFM,

FMI, FFMI, BMI, WC, SC, weight, AC, CC, and FC (Table 4.3) and had an  $R^2$  of 0.87 ( $r$ : 0.93, MSE: 0.220,  $p = 0.002$ ).

**Table 4.4** Combined models summary

	$\beta$ (95%CI)	$r$ ( $R^2$ )	p-value
<b>Total</b>			
BF%	0.12 (0.01, 0.22)	0.47 (0.22)	0.029
FM	0.12 (0.06, 0.34)	0.66 (0.43)	0.005
FMI	-0.91 (-1.44, -0.37)	0.63 (0.40)	0.001
FFMI	0.24 (0.07, 0.42)	0.57 (0.32)	0.006
Shoulder	-0.67 (-1.54, 0.20)	0.56 (0.31)	0.129
Chest	0.05 (-0.03, 0.13)	0.66 (0.43)	0.234
Biceps	-0.09 (-0.20, 0.03)	0.60 (0.36)	0.127
Stomach	-0.12 (-0.21, -0.03)	0.68 (0.46)	0.010
Hip	0.07 (0.02, 0.13)	0.63 (0.39)	0.013
WHt	25.61 (11.66, 39.56)	0.72 (0.52)	0.001
<b>Females</b>			
BF%	0.13 (0.02, 0.24)	0.72 (0.52)	0.026
FM	0.24 (0.05, 0.43)	0.68 (0.46)	0.016
FMI	-0.77 (-1.29, -0.25)	0.70 (0.49)	0.005
BSA	-0.01 (-0.11, -0.00)	0.59 (0.35)	0.002
Shoulder	-0.65 (-2.00, 0.70)	0.72 (0.72)	0.329
Chest	0.17 (0.06, 0.28)	0.74 (0.55)	0.004
Forearm	0.58 (0.25, 0.92)	0.67 (0.44)	0.001
Stomach	-0.02 (-0.11, 0.08)	0.72 (0.52)	0.730
WHR	-5.48 (-12.02, 1.06)	0.58 (0.34)	0.097
<b>Males</b>			
BF%	0.49 (0.14, 0.84)	0.63 (0.39)	0.011
FFM	-0.37 (-0.72, -0.02)	0.50 (0.25)	0.042
FMI	-0.92 (-1.69, -0.15)	0.66 (0.43)	0.024
FFMI	1.65 (0.51, 2.78)	0.62 (0.39)	0.008
Biceps	-1.10 (-1.87, -0.15)	0.54 (0.29)	0.009
Forearm	1.05 (-0.45, 2.54)	0.55 (0.31)	0.153
Stomach	-0.19 (-0.34, -0.04)	0.62 (0.38)	0.019
Hip	-0.56 (-1.30, 0.19)	0.64 (0.41)	0.131
Thigh	0.15 (-0.03, 0.33)	0.55 (0.30)	0.091
Calf	0.47 (-0.14, 1.09)	0.55 (0.30)	0.119
Waist	1.02 (0.20, 1.85)	0.65 (0.42)	0.019
WHR	-58.80 (-144.69, 27.10)	0.54 (0.30)	0.162
WHt	-49.22 (-134.45, 36.01)	0.66 (0.43)	0.232

Note: BF%, body fat percent; FM, fat mass; FMI, fat mass index; FFMI, fat-free mass index; WHt, waist-to-height

ratio; BSA, body surface area; FFM, fat-free mass; WHR, waist-to-hip ratio

#### 4.6 Prediction Equation Agreement Analysis

Prediction equations developed using body composition variables for the total sample produced a total error (TE) of 0.57 with limits of agreement (LOA) of  $\pm 1.12$ . Coefficients for the total sample indicated proportional bias; where MSs was underestimated with increasing MSs ( $\beta = -0.413$ ,  $p < 0.001$ ) (Figure 1.1).

Prediction equations developed using body composition variables for the female sample produced a TE of 0.58 with LOA of  $\pm 0.97$ . Coefficients for the total sample indicated proportional bias; where MSs was underestimated with increasing MSs ( $\beta = -0.375$ ,  $p = 0.008$ ) (Figure 1.2).

Prediction equations developed using body composition variables for the male sample produced a TE of 0.66 with LOA  $\pm 1.33$ . Coefficients for the total sample indicated proportional bias; where MSs was underestimated with increasing MSs ( $\beta = -0.492$ ,  $p = 0.010$ ) (Figure 1.3).

Figure 1.1 *Body Composition Total Model*

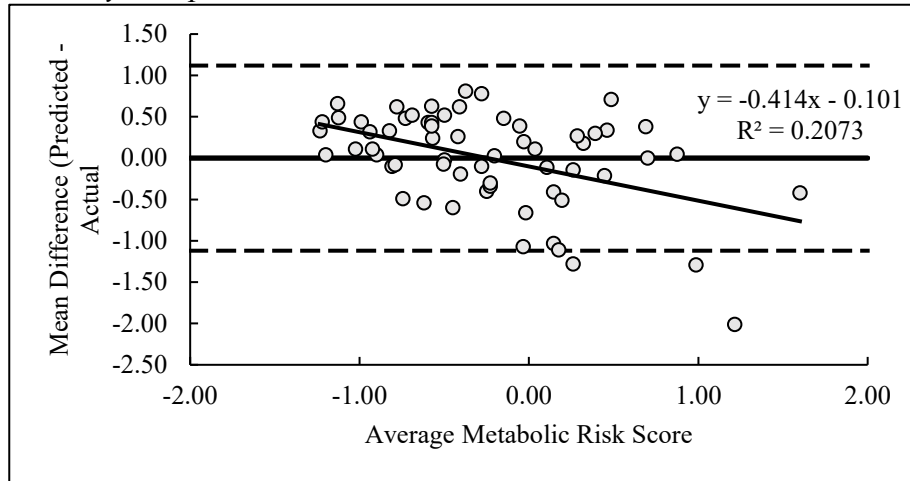


Figure 1.2 *Body Composition Female Model*

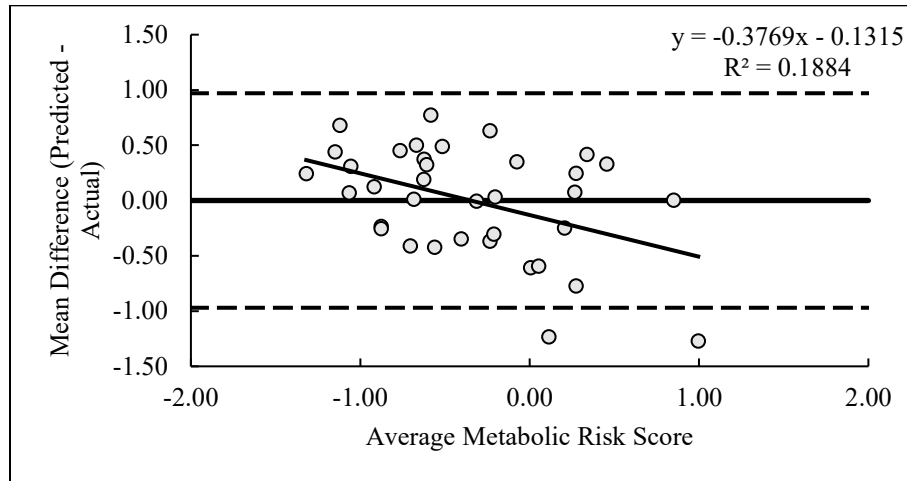
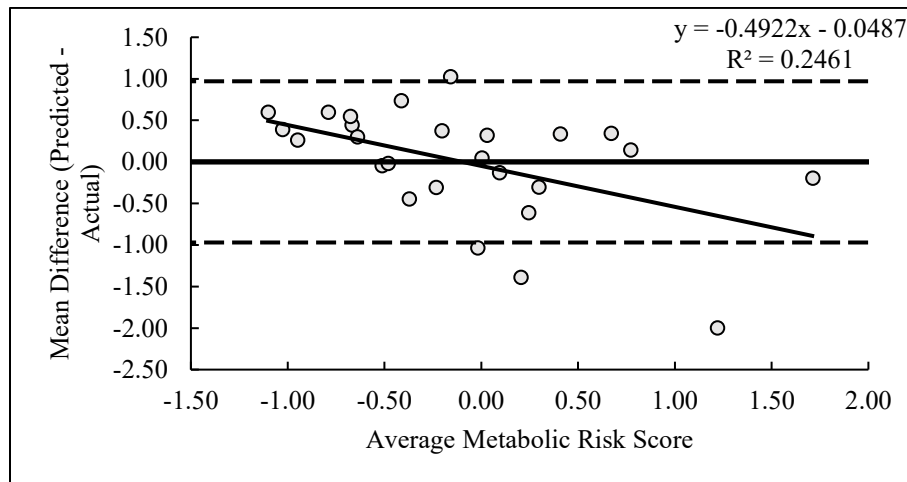


Figure 1.3 *Body Composition Male Model*



Prediction equations developed using anthropometric variables for the total sample produced a TE of 0.50 with LOA of  $\pm 0.99$ . Coefficients for the total sample indicated proportional bias; where MSs was underestimated with increasing MSs ( $\beta = -0.285$ ,  $p = 0.002$ ) (Figure 1.4).

Prediction equations developed using anthropometric variables for the female sample produced TE of 0.42 with LOA of  $\pm 0.84$ . Coefficients for the total sample indicated proportional bias; where MSs was underestimated with increasing MSs ( $\beta = -0.245$ ,  $p = 0.036$ ) (Figure 1.5).

Prediction equations developed using anthropometric variables for the male sample produced a TE of 0.46 with LOA of  $\pm 0.93$ . Coefficients for the total sample indicated no proportional bias ( $\beta = -0.175$ ,  $p = 0.142$ ) (Figure 1.6).

Figure 1.4 *Anthropometric Total Model*

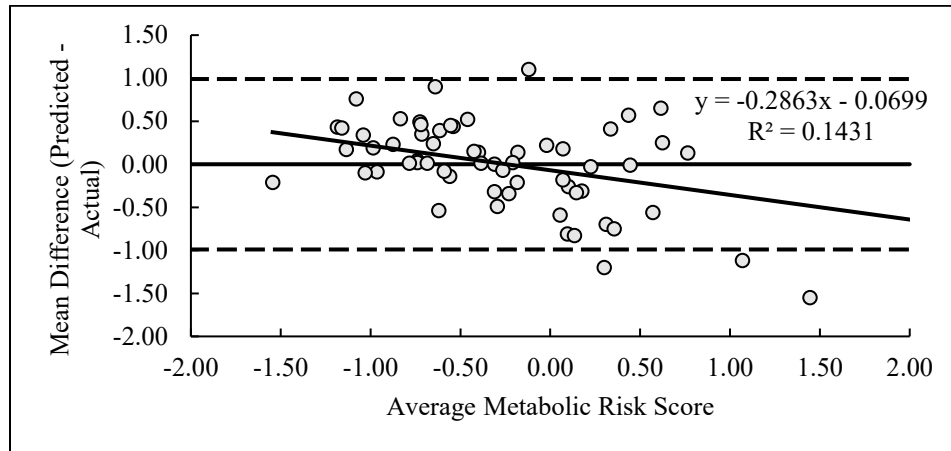


Figure 1.5 *Anthropometric Female Model*

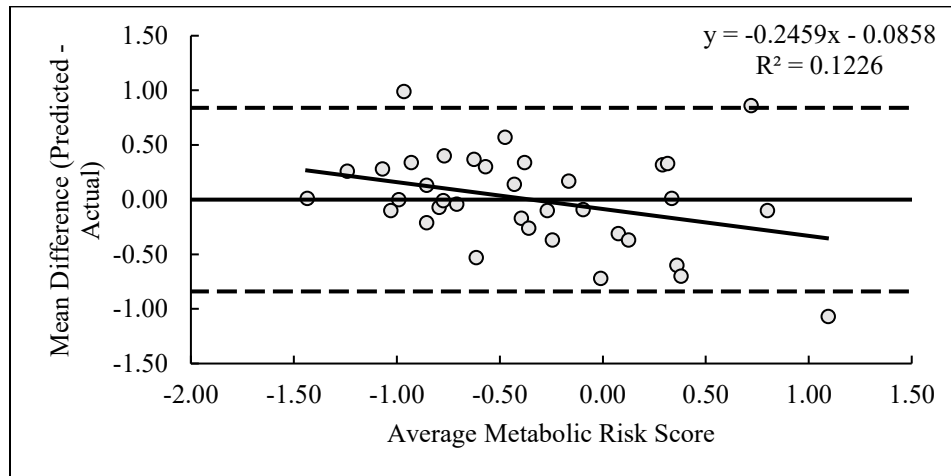
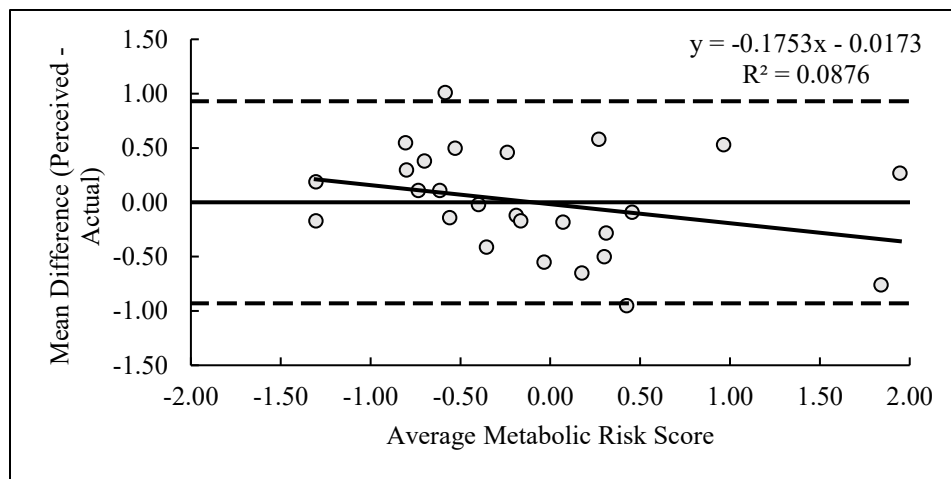


Figure 1.6 *Anthropometric Male Model*



Prediction equations developed using all variables for the total sample produced a TE of 0.47 and LOA that ranged from -0.94 to 0.94. Coefficients for the total sample indicated proportional bias; where MSs was underestimated with increasing MSs ( $\beta = -0.243$ ,  $p = 0.005$ ) (Figure 1.7).

Prediction equations developed using all variables for the female sample produced a TE of 0.34 and LOA that ranged from -0.67 to 0.67. Coefficients for the total sample indicated no presence of proportional bias ( $\beta = -0.137$ ,  $p = 0.123$ ) (Figure 1.8).

Prediction equations developed using all variables for the male sample produced TE of 0.32 and LOA that ranged from -0.64 to 0.64. Coefficients for the total sample indicated no presence of proportional bias ( $\beta = -0.072$ ,  $p = 0.142$ ) (Figure 1.9).



Figure 1.7 *Combined Variables - Total Model*

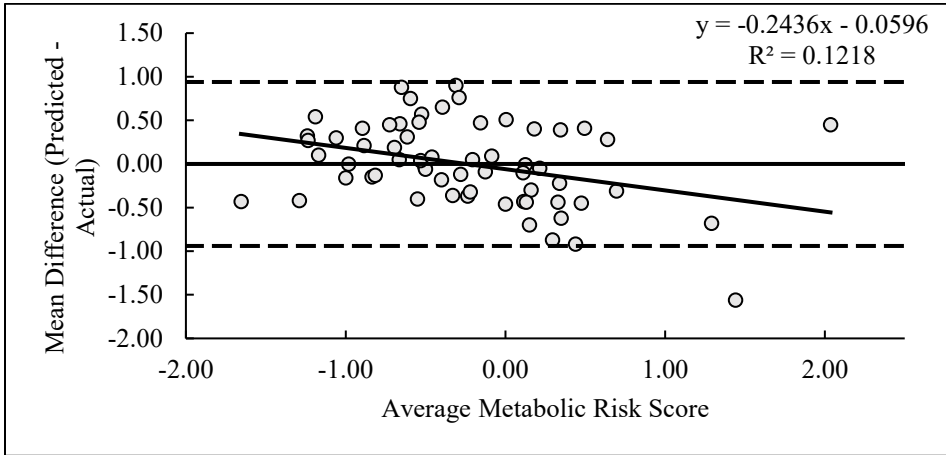


Figure 1.8 *Combined Variables - Female Model*

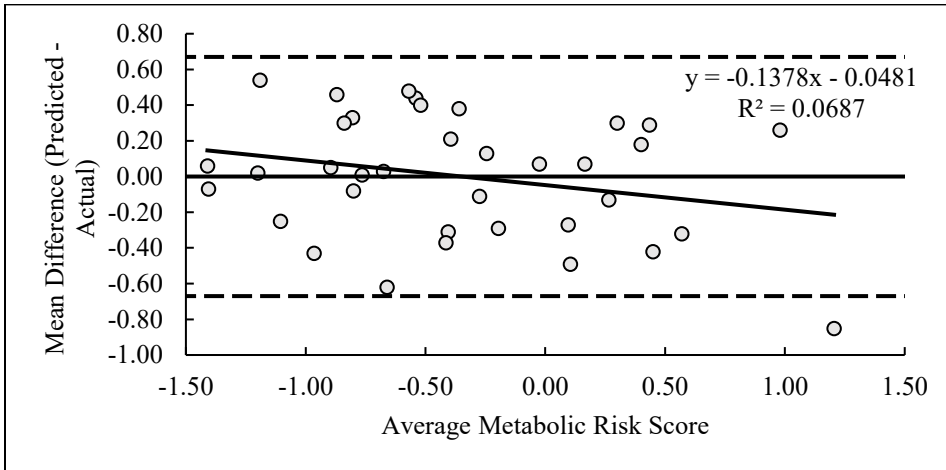
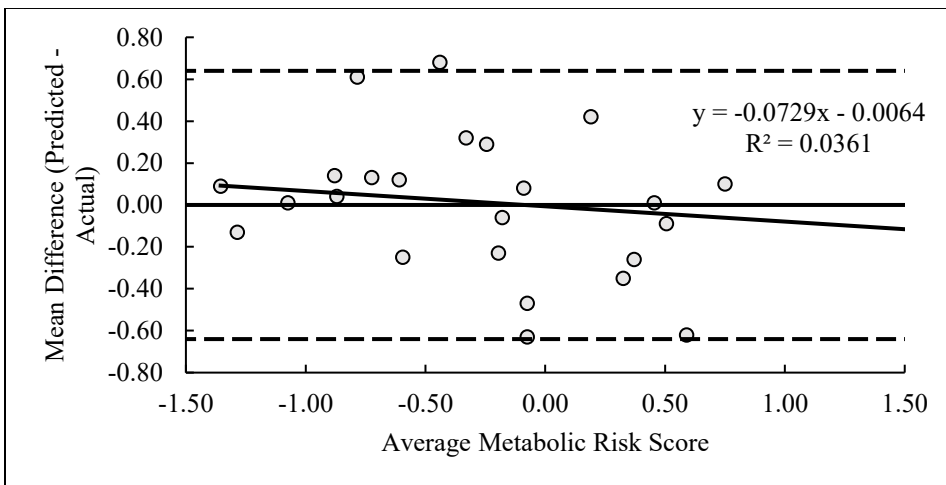


Figure 1.9 *Combined Variables - Male Model*



## CHAPTER V – DISCUSSION

This study sought to determine the predictive ability of a validated M-3DO application for predicting metabolic health risk as defined by an existing continuous MSs score<sup>192</sup>. While investigations from our laboratory and others have demonstrated the accuracy of M-3DO scanning techniques for both body composition and whole-body anthropometrics, there are no studies, to our knowledge, that have utilized M-3DO to evaluate a constellation of chronic disease risk factors; evaluations that would typically require in-person medical screening visits. Given that impairments in cardiometabolic health are typically obesity-driven, our study showed that M-3DO methods that can leverage this relationship (body size and cardiometabolic health risk) may offer utility in the prediction of cardiometabolic health status. While other laboratory and field based methods of health screening have also been shown to predict markers of cardiometabolic health<sup>193,194</sup>, this study is unique in that it may be the first body composition method equipped to provide these assessments remotely regardless of geographical location and without the need for additional devices, or a trained technician, which is invaluable now that increasing remote healthcare assessments are becoming a hallmark of improving access to diagnostic care. As such, the primary findings of the current investigation were:

- 1) All linear models demonstrated utility in the prediction of MSs, although models including both anthropometric and body composition components led to collective improvements in model performance;
- 2) Prediction models that were sex specific, compared to models that jointly included both males and females, resulted in model improvement; also demonstrating improvements in proportional bias on most occasions;
- 3) Body composition and anthropometric components retained in the models varied by

sex, likely due to the differential contributions of these body composition components on cardiometabolic disease risks between males and females. The findings of this investigation indicate that M-3DO derived measurements of body composition and anthropometry may offer utility in evaluating cardiometabolic health risk; particularly for those in rural or low SES communities with limited access to traditional metabolic health screening.

While BMI is broadly used for the evaluation of obesity and obesity-related cardiometabolic health risks, there are sizeable limitations to this approach, where more comprehensive metrics may provide better insight. As such, a major component of our study design was to determine the utility of a previously validated M-3DO body composition assessment method in the prediction of MSs. For the final prediction equations produced by our body composition specific models in the total sample, only BF% and FFMI were retained; accounting for 47%-57% of the variance in MSs. Interestingly, both metrics demonstrated significant and positive coefficients indicating that both were positively associated with MSs. While studies show that increasing BF% is associated with worsening cardiometabolic health, the inclusion of FFMI is noteworthy, given that FFM is generally considered to be more protective of metabolic health risks<sup>195</sup>. At the extremes of obesity, FFM increases concurrent with increases in FM and thus, it is likely that the inclusion of FFMI in the current model is more representative of overall body size which would, theoretically, increase cardiometabolic disease risk. Further insight to this may be revealed in our sex specific body composition models, which showed that the female model retained only BF% while the male model retained only FMI. Because, mathematically, FMI and FFMI are the residuals of each

other in regard to total body weight, it is possible that, in the total model, covariance in these components resulted in the elimination of one of these variables; with the eliminated variable being FMI. Although FMI would typically be more indicative of metabolic disease risk compared to FFMI, FMI was likely eliminated due to the similar absolute FM that existed between males and females. Because FFM is likely more protective of metabolic health risk, and because males have a greater capacity to gain FFM compared to females, it is likely that FFMI was included in the model for the total sample because females (who have a lower capacity to gain FFM) with excessive FFM similar to that of their male counterparts likely experience this as a function of larger overall body size which would, at some point, blunt the protective effects of FFM. Thus, when sex specific equations were generated, the models may have been able to detect the more deleterious effects of FM.

Circumference measurements such as WC, HC, WHR, and WHt are commonly used to evaluate cardiometabolic disease risk. Though useful, the measures' central focus may omit other potentially impactful anthropometric measures indicative of larger body size. Segmental anthropometrics require additional measures not often captured in normal health screening, but the further delineation of body segments (similar to DXA), such as specific truncal regions (i.e., chest, shoulders, stomach, etc.) and upper and lower appendages, may help to further identify cardiometabolic disease risks. Accordingly, another major component of our study was evaluating anthropometric measurements from the M-3DO application for the prediction of MSs. For the final prediction equations produced by our anthropometric specific model in the total sample, WHt, SC, HC, AC, FC, ChC, and SW were retained; accounting for 28%-52% of the variance in MSs.

Interestingly, all the variables included in the model were related to upper body anthropometrics, with the exception of HC and WHt. This is noteworthy given that in our final model for the total sample, HC was found to have a positive association with MSs. It is traditionally believed that adipose deposition favoring the gluteofemoral area is more protective of cardiometabolic disease development; yet the expected negative associations with HC were not observed in our model. This observation may suggest that there is a point where larger body sizes, indicated by greater HC and truncal measures that are associated with increased whole-body FM, renders the potential benefits of increased HC negligible; or, in more extreme cases of body size, to levels where HC becomes a positive risk factor. Increases in body size, composed of both FM and FFM, are traditionally reflected by increases in BMI, which itself is positively associated with cardiometabolic disease risks. However, this was not the case in our final female model, where BMI failed to demonstrate an expected positive association with MSs. When FM increases disproportionately in the absence of an elevated BMI (in regard to FFM during whole-body weight increase), the result is often a normal-weight obese phenotype; where individuals present with normal weight but, due to elevated FM and low FFM, also present with increased cardiometabolic health risks similar to their obese counterparts<sup>21,196</sup>. Thus, it is possible that BMI was included due to the disproportionate overlap between BMI and FM accretion, evident by the inclusion of BF% in the female body composition model. This may also be why BMI was included in the male model, however, the retention of specific variables not retained for females (i.e., upper body measures) may be more indicative of increases in FFM rather than FM. This may be supported by the observation that the male group in this study had a mean BMI higher

than the female group despite that HC and FM were similar between the sex groups. Additional variables included in the male model were WC, SC, weight, AC, CC, and FC. In males, increased biceps size is most likely associated with increased lean body mass which is demonstrated by the negative association with MSs. Interestingly, while AC was negatively associated with MSs, FC was positively associated with MSs. Previous studies have shown that FC is positively associated with MetS, especially in the presence of obesity<sup>197</sup>. Overall, these data showed that sex specific equations were able to better detect the health risks associated with the distinct anthropometric characteristics of males and females and highlight the importance of creating sex specific prediction models in the context of chronic disease risk.

Although body composition and anthropometric measures have well-demonstrated associations with cardiometabolic risk factors, there are inherent strengths and weaknesses associated with both approaches<sup>194</sup>. Thus, combining both measures should, theoretically, rectify the weaknesses of each, providing the most robust assessment. Accordingly, for the final model, including both sets of variables was able to account for the unique effects of both whole-body and regional measures. The combined model in the total sample included the variables BF%, FM, FMI, FFMI, SW, ChC, AC, SC, HC, and WHt; each accounting for 22% - 52% of variance in MSs. FM, FFMI, HC and WHt were all positively associated with MSs, of which all but FM were observed in the prior models, suggesting that when males and females are grouped these variables exert a unique effect on MetS. Further, AC was associated with lower MSs in the total model; yet, when divided by sex-group, these variables remained in the male model only. Together, the findings suggest that the disproportionate upper body adipose deposition,

which may occur in tandem with increased FFM, may attenuate the protective benefits of FFM. FM and BF% remained strong positive predictors of MSs, but the role of FMI may largely depend on body fat distribution which becomes more apparent within the sex-specific models. Among differences between the models, ChC was included within the female model which is notable as for females, increases in BMI and WC are associated with breast size and VAT<sup>198</sup> and in whom upper body adiposity is more detrimental to cardiometabolic health than in males<sup>199,200</sup>. The female model also retained FM and BSA which may both be attributable to higher BF (which has a greater volume by weight than FFM) that is commonly observed in females<sup>201</sup>. For males, the central measures of WHt and WC were likely retained given that the FM distribution around the abdomen, which is typical for males, is associated with increased abdominal VAT and metabolic health risk<sup>23</sup>. Notably, of the appendicular circumferences, only AC was negatively associated with MSs while FC, TC, and CC had a positive association. Among those variables, AC was the strongest negative predictor, and, as previously mentioned, is likely more representative of total body FFM and its protective effects against cardiometabolic health risks. Similar to the positive relationship observed between HC and MSs in the total anthropometric model, the inclusion of TC and CC as positive predictors in the male model may be due to larger body sizes that are more reflective of greater FM accumulation at the extremes of body size. Ultimately, the combination of body composition and anthropometric variables in conjunction with sex-specific equations allows regression models to provide the strongest equations for the prediction of MSs; as was observed in the present study.

Considering the variance accounted for by each of the aforementioned models, there is sound reason to hypothesize that these smartphone-based techniques are highly predictive of MetS. As such, our study sought to determine the predictive capacity of this technique to determine its utility in remote-diagnostic care. The performance of our prediction equations differed across model types and by sex within each model type. For the total models, TE was lowest in the combined model ( $\pm 0.47$ ) followed by the anthropometric ( $\pm 0.50$ ) and body composition models ( $\pm 0.57$ ). Similarly, the combined total model had the lowest, albeit high, LOA ( $\pm 0.94$ ) followed by the anthropometric and body composition models ( $\pm 0.99$  and  $\pm 1.12$ , respectively). All total models demonstrated significant proportional bias where, as body size increased, MSs was underestimated. The largest proportional bias was observed with the body composition model ( $\beta = -0.413$ ,  $p < 0.001$ ), followed by the anthropometric and combined models ( $\beta = -0.285$ ,  $p = 0.002$ , and  $\beta = -0.243$ ,  $p = 0.005$ , respectively). For the total models, the performance of the models improved with the number of variables included. The additional variables included likely helped the models account for more of the variation between the males and females within the models, whereas with less variables, as seen in the body composition model, sex differences had to be reduced to the lowest common similarity to fit the model. Interestingly, for the sex-specific body composition and anthropometric models, the total number of variables retained were either less or the same as the total models; where the variables retained may have better accounted for the variances between sex-groups. The sex-specific body composition model yielded improvements in the female model, though proportional bias remained significant (TE =  $\pm 0.58$ , LOA =  $\pm 0.97$ ,  $\beta = -0.375$ ,  $p = 0.008$ ), while decrements in the male model performance were observed (TE =  $\pm 0.66$ , LOA =



$\pm 1.33$ ,  $\beta = -0.492$ ,  $p = 0.01$ ). For the male model, more participants fell below the lower LOA with greater outliers than the female model. Those presenting with higher MSs but smaller body size likely accounted for the higher LOA and increased proportional bias, especially with nearly all body sizes above the median falling within the LOA. For the sex-specific anthropometric models, TE and LOA were improved for both the female ( $\pm 0.542$  and  $\pm 0.84$ ) and male models ( $\pm 0.46$  and  $\pm 0.93$ ), while only the male model observed non-significant proportional bias ( $\beta = -0.175$ ,  $p = 0.142$ ). As previously discussed, the presence of normal-weight obesity may have resulted in the observed proportional bias. Among females, 78% were normal or overweight compared to 53% among males; yet FM was not distinguishable between the two groups. The sex-specific combined models yielded the lowest TE (female:  $\pm 0.34$ , male:  $\pm 0.32$ ) and LOA (female:  $\pm 0.67$ , male:  $\pm 0.64$ ). Further, when divided by sex, the proportional bias within the models were no longer significant (male:  $\beta = -0.072$ ,  $p = 0.142$ , female:  $\beta = -0.137$ ,  $p = 0.123$ ). The reduction of proportional bias within the female combined model may be attributable to the combination of body composition variables, which capture more information on health risk than BMI and anthropometric measures alone. This observation may indicate where the distribution of excess FM is occurring and the role that it has on cardiometabolic health.

There are several strengths and limitations of the current study that warrant discussion. First, our study included a relatively small number of participants. Despite this, the models produced in the current study were able to significantly predict MSs; accounting for a large portion of the variance in MSs. Our sample also included a broad range of body compositions and degrees of metabolic health risk, where we had an

overweight and obesity prevalence of 70%, with 19% having at least three MetS risk factors and 48.2% having one to two risk factors. Our study also had an uneven distribution of races and ethnicities, particularly for Asian (3%) and Hispanic (13%) participants. However, our study had a more representative sample of Black/AA participants (26%), amounting to a combined 41% racial/ethnic minority sample. There are also potential limitations within the MSs equation. For instance, only SBP is included in the equation despite that DBP is a MetS classification criteria and that DBP may independently predict adverse cardiovascular outcomes<sup>202</sup>. However, considering that SBP and DBP share a strong linear relationship, it is likely that elevated DBP was, in part, reflected in the SBP values included in the equation. In addition to the inclusion of TG, a strong predictor of CVD risk<sup>203</sup>, HDL was included as a predictor variable. HDL is commonly considered a negative risk factor for CVD, and increased HDL levels are associated atherosclerosis regression<sup>204</sup>. However, the risk associated with HDL may not capture the full picture of health risk when TC levels are excessively high or low; as the HDL quality may be altered, exerting a more pro-inflammatory, pro-atherosclerotic effect<sup>205</sup>. The MSs equation also does not actively account for medication use, thus reducing the impact that a controlled risk factor has on the MSs score. Development of the equation used for MSs calculation was developed in healthy individuals, though it was cross-validated in individuals with known disease which may support its use for individuals of worsened health status<sup>192</sup>. In regard to our methodology, we used a single smartphone to produce our equations which may result in error if these equations are employed on different smartphones; however, measurements produced by the MeThreeSixty<sup>®</sup> application demonstrate acceptable reliability across smartphone types<sup>206</sup>,

and our study demonstrated the reliability between smartphone and tablet based systems. Our study also employed scanning procedures that followed manufacturer guidelines and were closely monitored by investigators, which may not be the technique employed outside of a laboratory setting. However, assuming that patient information is accurately uploaded, and the instructions provided prior to initiation of the scan are followed, the device should theoretically demonstrate acceptable accuracy outside of a laboratory setting; although more research is necessary to determine the validity of this technique outside of a research environment where it will likely be employed.

In conclusion, the findings of this study provide preliminary evidence for the potential of 3DO smartphone technology as a novel, accessible, and easy to use tool that can be employed for remote health screening. As telemedicine aims to bridge the gap between physicians and patients, the emergence of user-friendly, at-home screening tools signifies a significant stride in narrowing the healthcare access gap. 3DO scanning technology can provide an efficient and remotely deployable tool for health risk identification which can inform vital healthcare interventions. Such innovative tools hold immense promise in promoting improved health outcomes for individuals and communities alike.

## APPENDIX A – IRB Approval Letter

### Office of Research Integrity



118 COLLEGE DRIVE #5116 • HATTIESBURG, MS | 601.266.6756 | WWW.USM.EDU/ORI

#### NOTICE OF INSTITUTIONAL REVIEW BOARD ACTION

The project below has been reviewed by The University of Southern Mississippi Institutional Review Board in accordance with Federal Drug Administration regulations (21 CFR 26, 111), Department of Health and Human Services regulations (45 CFR Part 46), and University Policy to ensure:

- The risks to subjects are minimized and reasonable in relation to the anticipated benefits.
- The selection of subjects is equitable.
- Informed consent is adequate and appropriately documented.
- Where appropriate, the research plan makes adequate provisions for monitoring the data collected to ensure the safety of the subjects.
- Where appropriate, there are adequate provisions to protect the privacy of subjects and to maintain the confidentiality of all data.
- Appropriate additional safeguards have been included to protect vulnerable subjects.
- Any unanticipated, serious, or continuing problems encountered involving risks to subjects must be reported immediately. Problems should be reported to ORI via the Incident submission on InfoEd IRB.
- The period of approval is twelve months. An application for renewal must be submitted for projects exceeding twelve months.

PROTOCOL NUMBER: 22-1012

PROJECT TITLE: Examining the Cardiometabolic and Cardiorespiratory Outcomes of Metabolic Syndrome Phenotypes (ECCO-MSP)

SCHOOL/PROGRAM Kinesiology

RESEARCHERS: PI: Jonathon Stavres  
Investigators: Stavres, Jonathon~Graybeal, Austin~Galloway, Riley~Brandner, Caleb~Stanfield, Davion~Henderson, Alex~Haynes, Hunter~Parnell, Sarah~Faremi, Boluwatife~Renna, Megan~Behringer, Kylee~Aultman, Ryan~Newsome, Ta'Quoris~

IRB COMMITTEE ACTION: Approved

CATEGORY: Full Board Review

PERIOD OF APPROVAL: 17-Nov-2022 to 16-Nov-2023

Donald Sacco, Ph.D.  
Institutional Review Board Chairperson

## REFERENCES

1. Clinical Guidelines on the Identification, Evaluation, and Treatment of Overweight and Obesity in Adults--The Evidence Report. National Institutes of Health. *Obesity Research*. 1998;6(6). Accessed July 6, 2022. <https://onlinelibrary.wiley.com/doi/abs/10.1002/j.1550-8528.1998.tb00690.x?sid=nlm%3Apubmed>
2. Prospective Studies Collaboration. Body-mass index and cause-specific mortality in 900 000 adults: collaborative analyses of 57 prospective studies. *Lancet*. 2009;373(9669):1083-1096. doi:10.1016/S0140-6736(09)60318-4
3. Malnick SDH, Knobler H. The medical complications of obesity. *QJM: An International Journal of Medicine*. 2006;99(9):565-579. doi:10.1093/qjmed/hcl085
4. Hales CM. Prevalence of Obesity and Severe Obesity Among Adults: United States, 2017–2018. 2020;(360):8.
5. Cawley J, Biener A, Meyerhoefer C, et al. Direct medical costs of obesity in the United States and the most populous states. *JMCP*. 2021;27(3):354-366. doi:10.18553/jmcp.2021.20410
6. Ortega FB, Sui X, Lavie CJ, Blair SN. Body Mass Index, the Most Widely Used But Also Widely Criticized Index. *Mayo Clinic Proceedings*. 2016;91(4):443-455. doi:10.1016/j.mayocp.2016.01.008
7. Rinehart CS, Oliver JS. A Clinical Protocol for the Assessment of Obesity: Addressing an Epidemic. *Nursing Clinics of North America*. 2015;50(3):605-611. doi:10.1016/j.cnur.2015.05.013
8. Wajchenberg BL. Subcutaneous and Visceral Adipose Tissue: Their Relation to the Metabolic Syndrome. *Endocrine Reviews*. 2000;21(6):697-738. doi:10.1210/edrv.21.6.0415
9. Wong JC, O'Neill S, Beck BR, Forwood MR, Khoo SK. Comparison of obesity and metabolic syndrome prevalence using fat mass index, body mass index and percentage body fat. *PLOS ONE*. 2021;16(1):e0245436. doi:10.1371/journal.pone.0245436
10. Oh YH, Choi S, Lee G, Son JS, Kim KH, Park SM. Changes in Body Composition Are Associated with Metabolic Changes and the Risk of Metabolic Syndrome. *J Clin Med*. 2021;10(4):745. doi:10.3390/jcm10040745
11. Huang PL. A comprehensive definition for metabolic syndrome. *Dis Model Mech*. 2009;2(5-6):231-237. doi:10.1242/dmm.001180

12. Hirode G, Wong RJ. Trends in the Prevalence of Metabolic Syndrome in the United States, 2011-2016. *JAMA*. 2020;323(24):2526-2528. doi:10.1001/jama.2020.4501
13. Jensen MD, Ryan DH, Apovian CM, et al. 2013 AHA/ACC/TOS Guideline for the Management of Overweight and Obesity in Adults. *Journal of the American College of Cardiology*. 2014;63(25):2985-3023. doi:10.1016/j.jacc.2013.11.004
14. Welborn TA, Dhaliwal SS. Preferred clinical measures of central obesity for predicting mortality. *Eur J Clin Nutr*. 2007;61(12):1373-1379. doi:10.1038/sj.ejcn.1602656
15. Janssen I, Katzmarzyk PT, Ross R. Waist circumference and not body mass index explains obesity-related health risk. *Am J Clin Nutr*. 2004;79(3):379-384. doi:10.1093/ajcn/79.3.379
16. Patel P, Abate N. Body Fat Distribution and Insulin Resistance. *Nutrients*. 2013;5(6):2019-2027. doi:10.3390/nu5062019
17. Meisinger C, Döring A, Thorand B, Heier M, Löwel H. Body fat distribution and risk of type 2 diabetes in the general population: are there differences between men and women? The MONICA/KORA Augsburg Cohort Study 1985-1998. Published online December 1, 2006:7.
18. Gadekar T, Dudeja P, Basu I, Vashisht S, Mukherji S. Correlation of visceral body fat with waist-hip ratio, waist circumference and body mass index in healthy adults: A cross sectional study. *Med J Armed Forces India*. 2020;76(1):41-46. doi:10.1016/j.mjafi.2017.12.001
19. Kuk JL, Katzmarzyk PT, Nichaman MZ, Church TS, Blair SN, Ross R. Visceral fat is an independent predictor of all-cause mortality in men. *Obesity (Silver Spring)*. 2006;14(2):336-341. doi:10.1038/oby.2006.43
20. Cameron AJ, Romaniuk H, Orellana L, et al. Combined Influence of Waist and Hip Circumference on Risk of Death in a Large Cohort of European and Australian Adults. *J Am Heart Assoc*. 2020;9(13):e015189. doi:10.1161/JAHA.119.015189
21. Sahakyan KR, Somers VK, Rodriguez-Escudero JP, et al. Normal Weight Central Obesity: Implications for Total and Cardiovascular Mortality. *Ann Intern Med*. 2015;163(11):827-835. doi:10.7326/M14-2525
22. Nuttall FQ. Body Mass Index: Obesity, BMI, and Health A Critical Review. *Nutrition Today*. 2015;50(3):117-128. doi:10.1097/NT.0000000000000092
23. Tchernof A, Després JP. Pathophysiology of Human Visceral Obesity: An Update. *Physiological Reviews*. 2013;93(1):359-404. doi:10.1152/physrev.00033.2011

24. Kouchi M, Mochimaru M. Errors in landmarking and the evaluation of the accuracy of traditional and 3D anthropometry. *Applied Ergonomics*. 2011;42(3):518-527. doi:10.1016/j.apergo.2010.09.011
25. Peltz G, Aguirre MT, Sanderson M, Fadden MK. The role of fat mass index in determining obesity. *Am J Hum Biol*. 2010;22(5):639-647. doi:10.1002/ajhb.21056
26. Frankenfield DC, Rowe WA, Cooney RN, Smith JS, Becker D. Limits of body mass index to detect obesity and predict body composition. *Nutrition*. 2001;17(1):26-30. doi:10.1016/S0899-9007(00)00471-8
27. Müller MJ, Lagerpusch M, Enderle J, Schautz B, Heller M, Bosy-Westphal A. Beyond the body mass index: tracking body composition in the pathogenesis of obesity and the metabolic syndrome. *Obesity Reviews*. 2012;13(S2):6-13. doi:10.1111/j.1467-789X.2012.01033.x
28. Wijayatunga NN, Dhurandhar EJ. Normal weight obesity and unaddressed cardiometabolic health risk-a narrative review. *Int J Obes (Lond)*. 2021;45(10):2141-2155. doi:10.1038/s41366-021-00858-7
29. Beijers HJBH, Ferreira I, Bravenboer B, et al. Higher central fat mass and lower peripheral lean mass are independent determinants of endothelial dysfunction in the elderly: The Hoorn study. *Atherosclerosis*. 2014;233(1):310-318. doi:10.1016/j.atherosclerosis.2013.12.002
30. Tinsley GM, Harty PS, Stratton MT, Smith RW, Rodriguez C, Siedler MR. Tracking changes in body composition: comparison of methods and influence of pre-assessment standardisation. *Br J Nutr*. Published online July 30, 2021:1-19. doi:10.1017/S0007114521002579
31. Cloetens L, Johansson-Persson A, Helgegren H, et al. Assessment of body composition in subjects with metabolic syndrome comparing single-frequency bioelectrical impedance analysis and bioelectrical spectroscopy. *Metab Syndr Relat Disord*. 2015;13(2):91-98. doi:10.1089/met.2014.0130
32. Rockamann RA, Dalton EK, Arabas JL, Jorn L, Mayhew JL. Validity of Arm-to-Arm BIA Devices Compared to DXA for Estimating % Fat in College Men and Women. *Int J Exerc Sci*. 2017;10(7):977-988.
33. Heymsfield SB, Bourgeois B, Ng BK, Sommer MJ, Li X, Shepherd JA. Digital anthropometry: a critical review. *Eur J Clin Nutr*. 2018;72(5):680-687. doi:10.1038/s41430-018-0145-7
34. Sobhiyeh S, Kennedy S, Dunkel A, et al. Digital anthropometry for body circumference measurements: Toward the development of universal three-dimensional optical system analysis software. *Obesity Science & Practice*. 2021;7(1):35-44. doi:10.1002/osp4.467

35. Tinsley GM, Moore ML, Benavides ML, Dellinger JR, Adamson BT. 3-Dimensional optical scanning for body composition assessment: A 4-component model comparison of four commercially available scanners. *Clinical Nutrition*. 2020;39(10):3160-3167. doi:10.1016/j.clnu.2020.02.008
36. Ng BK, Sommer MJ, Wong MC, et al. Detailed 3-dimensional body shape features predict body composition, blood metabolites, and functional strength: the Shape Up! studies. *The American Journal of Clinical Nutrition*. 2019;110(6):1316-1326. doi:10.1093/ajcn/nqz218
37. Majmudar MD, Chandra S, Yakkala K, et al. Smartphone camera based assessment of adiposity: a validation study. *NPJ Digit Med*. 2022;5:79. doi:10.1038/s41746-022-00628-3
38. The Pew Research Center. *Mobile Fact Sheet*.; 2021. Accessed July 18, 2022. <https://www.pewresearch.org/internet/fact-sheet/mobile/>
39. Fact Sheet: Telehealth | AHA. Published February 2019. Accessed July 18, 2022. <https://www.aha.org/factsheet/telehealth>
40. Xu T, Pujara S, Sutton S, Rhee M. Telemedicine in the Management of Type 1 Diabetes. *Prev Chronic Dis*. 2018;15:E13. doi:10.5888/pcd15.170168
41. Rathbone AL, Prescott J. The Use of Mobile Apps and SMS Messaging as Physical and Mental Health Interventions: Systematic Review. *J Med Internet Res*. 2017;19(8):e295. doi:10.2196/jmir.7740
42. Debon R, Coleone JD, Bellei EA, De Marchi ACB. Mobile health applications for chronic diseases: A systematic review of features for lifestyle improvement. *Diabetes & Metabolic Syndrome: Clinical Research & Reviews*. 2019;13(4):2507-2512. doi:10.1016/j.dsx.2019.07.016
43. Befort CA, Nazir N, Perri MG. Prevalence of Obesity Among Adults From Rural and Urban Areas of the United States: Findings From NHANES (2005–2008). *J Rural Health*. 2012;28(4):392-397. doi:10.1111/j.1748-0361.2012.00411.x
44. Rising rural body-mass index is the main driver of the global obesity epidemic in adults. *Nature*. 2019;569(7755):260-264. doi:10.1038/s41586-019-1171-x
45. Okobi OE, Ajayi OO, Okobi TJ, et al. The Burden of Obesity in the Rural Adult Population of America. *Cureus*. 13(6):e15770. doi:10.7759/cureus.15770
46. Ravussin E, Lillioja S, Anderson TE, Christin L, Bogardus C. Determinants of 24-hour energy expenditure in man. Methods and results using a respiratory chamber. *J Clin Invest*. 1986;78(6):1568-1578.



47. Piaggi P. Metabolic Determinants of Weight Gain in Humans. *Obesity (Silver Spring)*. 2019;27(5):691-699. doi:10.1002/oby.22456
48. Westerterp KR. Control of energy expenditure in humans. *Eur J Clin Nutr*. 2017;71(3):340-344. doi:10.1038/ejcn.2016.237
49. Pontzer H, Yamada Y, Sagayama H, et al. Daily energy expenditure through the human life course. *Science*. 2021;373(6556):808-812. doi:10.1126/science.abe5017
50. American College of Sports Medicine, Riebe D, Ehrman JK, Liguori G, Magal M, eds. *ACSM's Guidelines for Exercise Testing and Prescription*. Tenth edition. Wolters Kluwer; 2018.
51. Haskell WL, Lee IM, Pate RR, et al. Physical Activity and Public Health: Updated Recommendation for Adults from the American College of Sports Medicine and the American Heart Association. *Medicine & Science in Sports & Exercise*. 2007;39(8):1423-1434. doi:10.1249/mss.0b013e3180616b27
52. Pontzer H, Durazo-Arvizu R, Dugas LR, et al. Constrained Total Energy Expenditure and Metabolic Adaptation to Physical Activity in Adult Humans. *Current Biology*. 2016;26(3):410-417. doi:10.1016/j.cub.2015.12.046
53. Wing RR, Phelan S. Long-term weight loss maintenance. *Am J Clin Nutr*. 2005;82(1 Suppl):222S-225S. doi:10.1093/ajcn/82.1.222S
54. Redman LM, Heilbronn LK, Martin CK, et al. Metabolic and behavioral compensations in response to caloric restriction: implications for the maintenance of weight loss. *PLoS One*. 2009;4(2):e4377. doi:10.1371/journal.pone.0004377
55. Martin CK, Heilbronn LK, de Jonge L, et al. Effect of calorie restriction on resting metabolic rate and spontaneous physical activity. *Obesity (Silver Spring)*. 2007;15(12):2964-2973. doi:10.1038/oby.2007.354
56. Kim TJ, von dem Knesebeck O. Income and obesity: what is the direction of the relationship? A systematic review and meta-analysis. *BMJ Open*. 2018;8(1):e019862. doi:10.1136/bmjopen-2017-019862
57. Benusic M, Cheskin LJ. Obesity prevalence in large US cities: association with socioeconomic indicators, race/ethnicity and physical activity. *Journal of Public Health*. 2021;43(1):148-154. doi:10.1093/pubmed/fdz077
58. Salazar-Sepúlveda LL, Villarreal-Pérez JZ. Impact of diagnosis of overweight and obesity on weight management among hospitalized patients. *Obes Res Clin Pract*. 2019;13(2):164-167. doi:10.1016/j.orcp.2019.01.003

59. Shaw ML, Caffrey M. ASCO Spotlight With Randall A. Oyer, MD: Clinical Trials Must Be Accessible to Everyone. *Evidence-Based Oncology*. 2022;15(9):SP236-SP236.
60. Fink JT, Iii GLM, Singh M, Nelson DA, Walker RE, Cisler RA. Discordant Documentation of Obesity Body Mass Index and Obesity Diagnosis in Electronic Medical Records. *Journal of Patient-Centered Research and Reviews*. 2014;1(4):164-170. doi:10.17294/2330-0698.1037
61. Obesity and overweight. Accessed July 21, 2022. <https://www.who.int/news-room/fact-sheets/detail/obesity-and-overweight>
62. Levine DM, Linder JA, Landon BE. Characteristics of Americans With Primary Care and Changes Over Time, 2002-2015. *JAMA Intern Med*. 2020;180(3):463-466. doi:10.1001/jamainternmed.2019.6282
63. Schiller JS, Lucas JW, Peregoy JA. Summary health statistics for u.s. Adults: national health interview survey, 2011. *Vital Health Stat 10*. 2012;(256):1-218.
64. Savage DB, Petersen KF, Shulman GI. Disordered Lipid Metabolism and the Pathogenesis of Insulin Resistance. *Physiological Reviews*. 2007;87(2):507-520. doi:10.1152/physrev.00024.2006
65. Calanna S, Scicali R, Di Pino A, et al. Lipid and liver abnormalities in haemoglobin A1c-defined prediabetes and type 2 diabetes. *Nutrition, Metabolism and Cardiovascular Diseases*. 2014;24(6):670-676. doi:10.1016/j.numecd.2014.01.013
66. Ingram KH, Hill H, Moellering DR, et al. Skeletal Muscle Lipid Peroxidation and Insulin Resistance in Humans. *J Clin Endocrinol Metab*. 2012;97(7):E1182-E1186. doi:10.1210/jc.2011-2963
67. Deshpande AD, Harris-Hayes M, Schootman M. Epidemiology of Diabetes and Diabetes-Related Complications. *Phys Ther*. 2008;88(11):1254-1264. doi:10.2522/ptj.20080020
68. Feldman EL, Callaghan BC, Pop-Busui R, et al. Diabetic neuropathy. *Nat Rev Dis Primers*. 2019;5(1):42. doi:10.1038/s41572-019-0097-9
69. Ziegler D, Papanas N, Vinik AI, Shaw JE. Chapter 1 - Epidemiology of polyneuropathy in diabetes and prediabetes. In: Zochodne DW, Malik RA, eds. *Handbook of Clinical Neurology*. Vol 126. Diabetes and the Nervous System. Elsevier; 2014:3-22. doi:10.1016/B978-0-444-53480-4.00001-1
70. Yau JWY, Rogers SL, Kawasaki R, et al. Global Prevalence and Major Risk Factors of Diabetic Retinopathy. *Diabetes Care*. 2012;35(3):556-564. doi:10.2337/dc11-1909

71. Zheng Y, He M, Congdon N. The worldwide epidemic of diabetic retinopathy. *Indian J Ophthalmol.* 2012;60(5):428-431. doi:10.4103/0301-4738.100542
72. Armstrong DG, Boulton AJM, Bus SA. Diabetic Foot Ulcers and Their Recurrence. *N Engl J Med.* 2017;376(24):2367-2375. doi:10.1056/NEJMra1615439
73. Prompers L, Schaper N, Apelqvist J, et al. Prediction of outcome in individuals with diabetic foot ulcers: focus on the differences between individuals with and without peripheral arterial disease. The EURODIALE Study. *Diabetologia.* 2008;51(5):747-755. doi:10.1007/s00125-008-0940-0
74. Hall KD, Ayuketah A, Brychta R, et al. Ultra-processed diets cause excess calorie intake and weight gain: An inpatient randomized controlled trial of ad libitum food intake. *Cell Metab.* 2019;30(1):67-77.e3. doi:10.1016/j.cmet.2019.05.008
75. Sundström J, Lind L, Lampa E, et al. Weight gain and blood pressure. *J Hypertens.* 2020;38(3):387-394. doi:10.1097/HJH.0000000000002298
76. He FJ, Li J, MacGregor GA. Effect of longer term modest salt reduction on blood pressure: Cochrane systematic review and meta-analysis of randomised trials. *BMJ.* 2013;346:f1325. doi:10.1136/bmj.f1325
77. Grillo A, Salvi L, Coruzzi P, Salvi P, Parati G. Sodium Intake and Hypertension. *Nutrients.* 2019;11(9):1970. doi:10.3390/nu11091970
78. Diaz KM, Shimbo D. Physical Activity and the Prevention of Hypertension. *Curr Hypertens Rep.* 2013;15(6):659-668. doi:10.1007/s11906-013-0386-8
79. Bakker EA, Sui X, Brellenthin AG, Lee DC. Physical activity and fitness for the prevention of hypertension. *Curr Opin Cardiol.* 2018;33(4):394-401. doi:10.1097/HCO.0000000000000526
80. Zwald ML, Akinbami LJ, Fakhouri THI, Fryar CD. Prevalence of Low High-density Lipoprotein Cholesterol Among Adults, by Physical Activity: United States, 2011-2014. *NCHS Data Brief.* 2017;(276):1-8.
81. Global, regional, and national comparative risk assessment of 84 behavioural, environmental and occupational, and metabolic risks or clusters of risks for 195 countries and territories, 1990–2017: a systematic analysis for the Global Burden of Disease Study 2017. *Lancet.* 2018;392(10159):1923-1994. doi:10.1016/S0140-6736(18)32225-6
82. Schmieder RE, Messerli FH. Obesity Hypertension. *Medical Clinics of North America.* 1987;71(5):991-1001. doi:10.1016/S0025-7125(16)30822-7
83. Mikhail N, Golub MS, Tuck ML. Obesity and hypertension. *Progress in Cardiovascular Diseases.* 1999;42(1):39-58. doi:10.1016/S0033-0620(99)70008-3

84. Natsis M, Antza C, Doundoulakis I, Stabouli S, Kotsis V. Hypertension in Obesity: Novel Insights. *Current Hypertension Reviews*. 16(1):30-36.
85. Nakamura K, Fuster JJ, Walsh K. Adipokines: A link between obesity and cardiovascular disease. *J Cardiol*. 2014;63(4):250-259.  
doi:10.1016/j.jjcc.2013.11.006
86. Csongrádi É, Káplár M, Nagy B, et al. Adipokines as atherothrombotic risk factors in obese subjects: Associations with haemostatic markers and common carotid wall thickness. *Nutrition, Metabolism and Cardiovascular Diseases*. 2017;27(6):571-580.  
doi:10.1016/j.numecd.2017.02.007
87. Libby P, Theroux P. Pathophysiology of Coronary Artery Disease. *Circulation*. 2005;111(25):3481-3488. doi:10.1161/CIRCULATIONAHA.105.537878
88. Fernández-Sánchez A, Madrigal-Santillán E, Bautista M, et al. Inflammation, Oxidative Stress, and Obesity. *Int J Mol Sci*. 2011;12(5):3117-3132.  
doi:10.3390/ijms12053117
89. Engin A. Endothelial Dysfunction in Obesity. *Adv Exp Med Biol*. 2017;960:345-379.  
doi:10.1007/978-3-319-48382-5\_15
90. Ibanez B, Vilahur G, Badimon JJ. Plaque progression and regression in atherothrombosis. *Journal of Thrombosis and Haemostasis*. 2007;5(s1):292-299.  
doi:10.1111/j.1538-7836.2007.02483.x
91. Konukoglu D, Uzun H. Endothelial Dysfunction and Hypertension. *Adv Exp Med Biol*. 2017;956:511-540. doi:10.1007/5584\_2016\_90
92. Malakar AK, Choudhury D, Halder B, Paul P, Uddin A, Chakraborty S. A review on coronary artery disease, its risk factors, and therapeutics. *J Cell Physiol*. 2019;234(10):16812-16823. doi:10.1002/jcp.28350
93. Cecelja M, Chowienczyk P. Role of arterial stiffness in cardiovascular disease. *JRSM Cardiovascular Disease*. 2012;1(4):1-10. doi:10.1258/cvd.2012.012016
94. Badimon L, Vilahur G. Thrombosis formation on atherosclerotic lesions and plaque rupture. *J Intern Med*. 2014;276(6):618-632. doi:10.1111/joim.12296
95. Koga J ichiro, Aikawa M. Crosstalk between macrophages and smooth muscle cells in atherosclerotic vascular diseases. *Vascul Pharmacol*. 2012;57(1):24-28.  
doi:10.1016/j.vph.2012.02.011
96. Aikawa M, Libby P. The vulnerable atherosclerotic plaque: Pathogenesis and therapeutic approach. *Cardiovascular Pathology*. 2004;13(3):125-138.  
doi:10.1016/S1054-8807(04)00004-3

97. Gadde KM, Martin CK, Berthoud HR, Heymsfield SB. Obesity: Pathophysiology and Management. *J Am Coll Cardiol*. 2018;71(1):69-84. doi:10.1016/j.jacc.2017.11.011
98. Levy D. Clinical significance of left ventricular hypertrophy: insights from the Framingham Study. *J Cardiovasc Pharmacol*. 1991;17 Suppl 2:S1-6. doi:10.1097/00005344-199117002-00002
99. Zabalgoitia M, Berning J, Koren MJ, et al. Impact of coronary artery disease on left ventricular systolic function and geometry in hypertensive patients with left ventricular hypertrophy (the LIFE study). *American Journal of Cardiology*. 2001;88(6):646-650. doi:10.1016/S0002-9149(01)01807-0
100. Fletcher L, Thomas D. Congestive Heart Failure: Understanding the Pathophysiology and Management. *Journal of the American Academy of Nurse Practitioners*. 2001;13(6):249-257. doi:10.1111/j.1745-7599.2001.tb00030.x
101. Rogers C, Bush N. Heart Failure: Pathophysiology, Diagnosis, Medical Treatment Guidelines, and Nursing Management. *Nursing Clinics of North America*. 2015;50(4):787-799. doi:10.1016/j.cnur.2015.07.012
102. Tanai E, Frantz S. Pathophysiology of Heart Failure. In: *Comprehensive Physiology*. John Wiley & Sons, Ltd; 2015:187-214. doi:10.1002/cphy.c140055
103. Conte SM, Vale PR. Peripheral Arterial Disease. *Heart, Lung and Circulation*. 2018;27(4):427-432. doi:10.1016/j.hlc.2017.10.014
104. Virmani R, Burke AP, Farb A. Sudden cardiac death. *Cardiovascular Pathology*. 2001;10(5):211-218. doi:10.1016/S1054-8807(01)00091-6
105. Gongora-Rivera F, Labreuche J, Jaramillo A, Steg PG, Hauw JJ, Amarenco P. Autopsy Prevalence of Coronary Atherosclerosis in Patients With Fatal Stroke. *Stroke*. 2007;38(4):1203-1210. doi:10.1161/01.STR.0000260091.13729.96
106. Keller K, Hobohm L, Münzel T, Ostad MA. Impact of symptomatic atherosclerosis in patients with pulmonary embolism. *International Journal of Cardiology*. 2019;278:225-231. doi:10.1016/j.ijcard.2018.12.019
107. Khan F, Tritschler T, Kahn SR, Rodger MA. Venous thromboembolism. *The Lancet*. 2021;398(10294):64-77. doi:10.1016/S0140-6736(20)32658-1
108. Konstantinides SV, Barco S, Lankeit M, Meyer G. Management of Pulmonary Embolism: An Update. *J Am Coll Cardiol*. 2016;67(8):976-990. doi:10.1016/j.jacc.2015.11.061

109. Palmer MK, Toth PP. Trends in Lipids, Obesity, Metabolic Syndrome, and Diabetes Mellitus in the United States: An NHANES Analysis (2003-2004 to 2013-2014). *Obesity*. 2019;27(2):309-314. doi:10.1002/oby.22370
110. Engin A. The Definition and Prevalence of Obesity and Metabolic Syndrome. In: Engin AB, Engin A, eds. *Obesity and Lipotoxicity*. Advances in Experimental Medicine and Biology. Springer International Publishing; 2017:1-17. doi:10.1007/978-3-319-48382-5\_1
111. Hales CM, Fryar CD, Carroll MD, Freedman DS, Ogden CL. Trends in Obesity and Severe Obesity Prevalence in US Youth and Adults by Sex and Age, 2007-2008 to 2015-2016. *JAMA*. 2018;319(16):1723-1725. doi:10.1001/jama.2018.3060
112. Poesen K, De Prins M, Van den Berghe G, Van Eldere J, Vanstapel F. Performance of cassette-based blood gas analyzers to monitor blood glucose and lactate levels in a surgical intensive care setting. *Clin Chem Lab Med*. 2013;51(7):1417-1427. doi:10.1515/cclm-2012-0848
113. Nordestgaard BG, Varbo A. Triglycerides and cardiovascular disease. *The Lancet*. 2014;384(9943):626-635. doi:10.1016/S0140-6736(14)61177-6
114. Plüddemann A, Thompson M, Price CP, Wolstenholme J, Heneghan C. Point-of-care testing for the analysis of lipid panels: primary care diagnostic technology update. *Br J Gen Pract*. 2012;62(596):e224-e226. doi:10.3399/bjgp12X630241
115. Bundy JD, Li C, Stuchlik P, et al. Systolic Blood Pressure Reduction and Risk of Cardiovascular Disease and Mortality: A Systematic Review and Network Meta-analysis. *JAMA Cardiology*. 2017;2(7):775-781. doi:10.1001/jamacardio.2017.1421
116. Guerra RS, Amaral TF, Marques EA, Mota J, Restivo MT. Anatomical location for waist circumference measurement in older adults: a preliminary study. *Nutr Hosp*. 2012;27(5):1554-1561. doi:10.3305/nh.2012.27.5.5922
117. Ma WY, Yang CY, Shih SR, et al. Measurement of Waist Circumference: Midabdominal or iliac crest? *Diabetes Care*. 2013;36(6):1660-1666. doi:10.2337/dc12-1452
118. Abe M, Fujii H, Funakoshi S, et al. Comparison of Body Mass Index and Waist Circumference in the Prediction of Diabetes: A Retrospective Longitudinal Study. *Diabetes Therapy*. Published online 2021. doi:10.1007/s13300-021-01138-3
119. Snijder MB, Zimmet PZ, Visser M, Dekker JM, Seidell JC, Shaw JE. Independent and opposite associations of waist and hip circumferences with diabetes, hypertension and dyslipidemia: the AusDiab Study. *Int J Obes Relat Metab Disord*. 2004;28(3):402-409. doi:10.1038/sj.ijo.0802567

120. Yusuf S, Hawken S, Ôunpuu S, et al. Obesity and the risk of myocardial infarction in 27 000 participants from 52 countries: a case-control study. *The Lancet*. 2005;366(9497):1640-1649. doi:10.1016/S0140-6736(05)67663-5
121. Fosbøl MØ, Zerahn B. Contemporary methods of body composition measurement. *Clin Physiol Funct Imaging*. 2015;35(2):81-97. doi:10.1111/cpf.12152
122. Karstaedt N, Dixon RL, Wolfman NT, Ekstrand KE. Nuclear magnetic resonance imaging. *Surg Neurol*. 1983;19(3):206-214. doi:10.1016/s0090-3019(83)80003-2
123. Geva T. Magnetic resonance imaging: historical perspective. *J Cardiovasc Magn Reson*. 2006;8(4):573-580. doi:10.1080/10976640600755302
124. Bouazizi K, Zarai M, Dietenbeck T, et al. Abdominal adipose tissue components quantification in MRI as a relevant biomarker of metabolic profile. *Magnetic Resonance Imaging*. 2021;80:14-20. doi:10.1016/j.mri.2021.04.002
125. Karlsson A, Rosander J, Romu T, et al. Automatic and quantitative assessment of regional muscle volume by multi-atlas segmentation using whole-body water–fat MRI. *Journal of Magnetic Resonance Imaging*. 2015;41(6):1558-1569. doi:10.1002/jmri.24726
126. Alexander RE, Gunderman RB. EMI and the first CT scanner. *J Am Coll Radiol*. 2010;7(10):778-781. doi:10.1016/j.jacr.2010.06.003
127. Cantatore A, Müller P. *Introduction to Computed Tomography*. DTU Mechanical Engineering; 2011.
128. Hathcock JT, Stickle RL. Principles and Concepts of Computed Tomography. *Veterinary Clinics of North America: Small Animal Practice*. 1993;23(2):399-415. doi:10.1016/S0195-5616(93)50034-7
129. Xia Y, Ergun DL, Wacker WK, Wang X, Davis CE, Kaul S. Relationship Between Dual-Energy X-Ray Absorptiometry Volumetric Assessment and X-ray Computed Tomography–Derived Single-Slice Measurement of Visceral Fat. *Journal of Clinical Densitometry*. 2014;17(1):78-83. doi:10.1016/j.jocd.2013.03.007
130. Brenner DJ, Hall EJ. Computed Tomography — An Increasing Source of Radiation Exposure. *New England Journal of Medicine*. 2007;357(22):2277-2284. doi:10.1056/NEJMra072149
131. Cameron JR, Sorenson J. Measurement of Bone Mineral in vivo: An Improved Method. *Science*. 1963;142(3589):230-232. doi:10.1126/science.142.3589.230
132. Mazess RB, Peppler WW, Harrison JE, McNeill KG. Total body bone mineral and lean body mass by dual-photon absorptiometry. *Calcif Tissue Int*. 1981;33(1):365-368. doi:10.1007/BF02409457

133. Theodorou DJ, Theodorou SJ. Dual-energy X-ray absorptiometry in clinical practice: Application and interpretation of scans beyond the numbers. *Clinical Imaging*. 2002;26(1):43-49. doi:10.1016/S0899-7071(01)00356-4
134. Ackland TR, Lohman TG, Sundgot-Borgen J, et al. Current Status of Body Composition Assessment in Sport: Review and Position Statement on Behalf of the Ad Hoc Research Working Group on Body Composition Health and Performance, Under the Auspices of the I.O.C. Medical Commission. *Sports Medicine*. 2012;42(3):227-249. doi:10.2165/11597140-000000000-00000
135. Micklesfield LK, Goedecke JH, Punyanitya M, Wilson KE, Kelly TL. Dual-Energy X-Ray Performs as Well as Clinical Computed Tomography for the Measurement of Visceral Fat. *Obesity*. 2012;20(5):1109-1114. doi:10.1038/oby.2011.367
136. Neeland IJ, Grundy SM, Li X, Adams-Huet B, Vega GL. Comparison of visceral fat mass measurement by dual-X-ray absorptiometry and magnetic resonance imaging in a multiethnic cohort: the Dallas Heart Study. *Nutr Diabetes*. 2016;6(7):e221. doi:10.1038/nutd.2016.28
137. Mohammad A, De Lucia Rolfe E, Sleight A, et al. Validity of visceral adiposity estimates from DXA against MRI in Kuwaiti men and women. *Nutr Diabetes*. 2017;7(1):e238. doi:10.1038/nutd.2016.38
138. Prior BM, Cureton KJ, Modlesky CM, et al. In vivo validation of whole body composition estimates from dual-energy X-ray absorptiometry. *Journal of Applied Physiology*. 1997;83(2):623-630. doi:10.1152/jappl.1997.83.2.623
139. Sopher AB, Thornton JC, Wang J, Pierson RN Jr, Heymsfield SB, Horlick M. Measurement of Percentage of Body Fat in 411 Children and Adolescents: A Comparison of Dual-Energy X-Ray Absorptiometry With a Four-Compartment Model. *Pediatrics*. 2004;113(5):1285-1290. doi:10.1542/peds.113.5.1285
140. Lohman TG, Harris M, Teixeira PJ, Weiss L. Assessing body composition and changes in body composition. Another look at dual-energy X-ray absorptiometry. *Ann N Y Acad Sci*. 2000;904:45-54. doi:10.1111/j.1749-6632.2000.tb06420.x
141. Nana A, Slater GJ, Stewart AD, Burke LM. Methodology Review: Using Dual-Energy X-Ray Absorptiometry (DXA) for the Assessment of Body Composition in Athletes and Active People. *International Journal of Sport Nutrition and Exercise Metabolism*. 2015;25(2):198-215. doi:10.1123/ijsnem.2013-0228
142. Kim J, Wang Z, Heymsfield SB, Baumgartner RN, Gallagher D. Total-body skeletal muscle mass: estimation by a new dual-energy X-ray absorptiometry method. *The American Journal of Clinical Nutrition*. 2002;76(2):378-383. doi:10.1093/ajcn/76.2.378



143. Kim J, Shen W, Gallagher D, et al. Total-body skeletal muscle mass: estimation by dual-energy X-ray absorptiometry in children and adolescents. *The American Journal of Clinical Nutrition*. 2006;84(5):1014-1020. doi:10.1093/ajcn/84.5.1014
144. Miazgowski T, Krzyżanowska-Świniarska B, Dziwura-Ogonowska J, Widecka K. The associations between cardiometabolic risk factors and visceral fat measured by a new dual-energy X-ray absorptiometry-derived method in lean healthy Caucasian women. *Endocrine*. 2014;47(2):500-505. doi:10.1007/s12020-014-0180-7
145. Sasai H, Brychta RJ, Wood RP, et al. Does Visceral Fat Estimated by Dual-Energy X-ray Absorptiometry Independently Predict Cardiometabolic Risks in Adults? *J Diabetes Sci Technol*. 2015;9(4):917-924. doi:10.1177/1932296815577424
146. van der Ploeg GE, Withers RT, Laforgia J. Percent body fat via DEXA: comparison with a four-compartment model. *Journal of Applied Physiology*. 2003;94(2):499-506. doi:10.1152/jappphysiol.00436.2002
147. Williams JE, Wells JC, Wilson CM, Haroun D, Lucas A, Fewtrell MS. Evaluation of Lunar Prodigy dual-energy X-ray absorptiometry for assessing body composition in healthy persons and patients by comparison with the criterion 4-component model. *The American Journal of Clinical Nutrition*. 2006;83(5):1047-1054. doi:10.1093/ajcn/83.5.1047
148. Bone-Density Tests | Choosing Wisely. Promoting conversations between providers and patients. Published May 2012. Accessed September 19, 2022. <https://www.choosingwisely.org/patient-resources/bone-density-tests/>
149. Wang Z, Heshka S, Wang J, Wielopolski L, Heymsfield SB. Magnitude and variation of fat-free mass density: a cellular-level body composition modeling study. *American Journal of Physiology-Endocrinology and Metabolism*. 2003;284(2):E267-E273. doi:10.1152/ajpendo.00151.2002
150. Nickerson BS, Esco MR, Bishop PA, et al. Impact of Measured vs. Predicted Residual Lung Volume on Body Fat Percentage Using Underwater Weighing and 4-Compartment Model. *The Journal of Strength & Conditioning Research*. 2017;31(9):2519-2527. doi:10.1519/JSC.0000000000001698
151. Siri WE. The gross composition of the body. *Adv Biol Med Phys*. 1956;4:239-280. doi:10.1016/b978-1-4832-3110-5.50011-x
152. Brozek J, Grande F, Anderson JT, Keys A. DENSITOMETRIC ANALYSIS OF BODY COMPOSITION: REVISION OF SOME QUANTITATIVE ASSUMPTIONS. *Ann N Y Acad Sci*. 1963;110:113-140. doi:10.1111/j.1749-6632.1963.tb17079.x
153. Muntean P, Micloş-Balica M, Popa A, Neagu A, Neagu M. Reliability of Repeated Trials Protocols for Body Composition Assessment by Air Displacement

- Plethysmography. *Int J Environ Res Public Health*. 2021;18(20):10693. doi:10.3390/ijerph182010693
154. Vescovi JD, Zimmerman SL, Miller WC, Fernhall B. Effects of clothing on accuracy and reliability of air displacement plethysmography. *Med Sci Sports Exerc*. 2002;34(2):282-285. doi:10.1097/00005768-200202000-00016
155. Minderico CS, Silva AM, Teixeira PJ, Sardinha LB, Hull HR, Fields DA. Validity of air-displacement plethysmography in the assessment of body composition changes in a 16-month weight loss program. *Nutr Metab (Lond)*. 2006;3(1):32. doi:10.1186/1743-7075-3-32
156. Azcue M, Wesson D, Neuman M, Pencharz P. What does bioelectrical impedance spectroscopy (BIS) measure? *Basic Life Sci*. 1993;60:121-123. doi:10.1007/978-1-4899-1268-8\_27
157. Matias CN, Nunes CL, Francisco S, et al. Phase angle predicts physical function in older adults. *Archives of Gerontology and Geriatrics*. 2020;90:104151. doi:10.1016/j.archger.2020.104151
158. Stellingwerf F, Beumeler LFE, Rijnhart-de Jong H, Boerma EC, Buter H. The predictive value of phase angle on long-term outcome after ICU admission. *Clinical Nutrition*. 2022;41(6):1256-1259. doi:10.1016/j.clnu.2022.03.029
159. Hui D, Dev R, Pimental L, et al. Association between Multi-Frequency Phase Angle and Survival in Patients with Advanced Cancer. *J Pain Symptom Manage*. 2017;53(3):571-577. doi:10.1016/j.jpainsymman.2016.09.016
160. Kubo Y, Noritake K, Nakashima D, Fujii K, Yamada K. Relationship between nutritional status and phase angle as a noninvasive method to predict malnutrition by sex in older inpatients. *Nagoya J Med Sci*. 2021;83(1):31-40. doi:10.18999/nagjms.83.1.31
161. Yamada Y, Watanabe Y, Ikenaga M, et al. Comparison of single- or multifrequency bioelectrical impedance analysis and spectroscopy for assessment of appendicular skeletal muscle in the elderly. *Journal of Applied Physiology*. 2013;115(6):812-818. doi:10.1152/jappphysiol.00010.2013
162. Xu Z, Liu Y, Yan C, et al. Measurement of visceral fat and abdominal obesity by single-frequency bioelectrical impedance and CT: a cross-sectional study. *BMJ Open*. 2021;11(10):e048221. doi:10.1136/bmjopen-2020-048221
163. Park KS, Lee DH, Lee J, et al. Comparison between two methods of bioelectrical impedance analyses for accuracy in measuring abdominal visceral fat area. *Journal of Diabetes and its Complications*. 2016;30(2):343-349. doi:10.1016/j.jdiacomp.2015.10.014

164. Gába A, Kapuš O, Cuberek R, Botek M. Comparison of multi- and single-frequency bioelectrical impedance analysis with dual-energy X-ray absorptiometry for assessment of body composition in post-menopausal women: effects of body mass index and accelerometer-determined physical activity. *J Hum Nutr Diet.* 2015;28(4):390-400. doi:10.1111/jhn.12257
165. TAUBER RN, CAMIC CL, ZHANG S, CHOMENTOWSKI PJ. Comparison of Multi-Frequency Bioelectrical Impedance and Dual-Energy X-Ray Absorptiometry to Assess Body Composition in College-Aged Adults. *Int J Exerc Sci.* 2020;13(4):1595-1604.
166. Antonio J, Kenyon M, Ellerbroek A, et al. Comparison of Dual-Energy X-ray Absorptiometry (DXA) Versus a Multi-Frequency Bioelectrical Impedance (InBody 770) Device for Body Composition Assessment after a 4-Week Hypoenergetic Diet. *J Funct Morphol Kinesiol.* 2019;4(2):23. doi:10.3390/jfmk4020023
167. Schoenfeld BJ, Nickerson BS, Wilborn CD, et al. Comparison of Multifrequency Bioelectrical Impedance vs. Dual-Energy X-ray Absorptiometry for Assessing Body Composition Changes After Participation in a 10-Week Resistance Training Program. *J Strength Cond Res.* 2020;34(3):678-688. doi:10.1519/JSC.0000000000002708
168. Kyle UG, Bosaeus I, De Lorenzo AD, et al. Bioelectrical impedance analysis—part II: utilization in clinical practice. *Clinical Nutrition.* 2004;23(6):1430-1453. doi:10.1016/j.clnu.2004.09.012
169. Jackson AS, Pollock ML. Generalized equations for predicting body density of men. *Br J Nutr.* 1978;40(3):497-504. doi:10.1079/bjn19780152
170. Jackson AS, Pollock ML, Ward A. Generalized equations for predicting body density of women. *Med Sci Sports Exerc.* 1980;12(3):175-181.
171. Chambers AJ, Parise E, McCrory JL, Cham R. A Comparison of Prediction Equations for the Estimation of Body Fat Percentage in Non-obese and Obese Older Caucasian Adults in the United States. *J Nutr Health Aging.* 2014;18(6):586-590. doi:10.1007/s12603-014-0017-3
172. Deurenberg P, Deurenberg-Yap M. Validation of skinfold thickness and hand-held impedance measurements for estimation of body fat percentage among Singaporean Chinese, Malay and Indian subjects. *Asia Pac J Clin Nutr.* 2002;11(1):1-7. doi:10.1046/j.1440-6047.2002.00258.x
173. López-Taylor JR, González-Mendoza RG, Gaytán-González A, et al. Accuracy of Anthropometric Equations for Estimating Body Fat in Professional Male Soccer Players Compared with DXA. *Journal of Sports Medicine.* 2018;2018. doi:10.1155/2018/6843792

174. Peterson MJ, Czerwinski SA, Siervogel RM. Development and validation of skinfold-thickness prediction equations with a 4-compartment model. *Am J Clin Nutr.* 2003;77(5):1186-1191. doi:10.1093/ajcn/77.5.1186
175. Evans EM, Rowe DA, Mistic MM, Prior BM, Arngrímsson SÁ. Skinfold Prediction Equation for Athletes Developed Using a Four-Component Model. *Medicine & Science in Sports & Exercise.* 2005;37(11):2006-2011. doi:10.1249/01.mss.0000176682.54071.5c
176. Aandstad A, Holtberget K, Hageberg R, Holme I, Anderssen SA. Validity and Reliability of Bioelectrical Impedance Analysis and Skinfold Thickness in Predicting Body Fat in Military Personnel. *Military Medicine.* 2014;179(2):208-217. doi:10.7205/MILMED-D-12-00545
177. Majumder S, Deen MJ. Smartphone Sensors for Health Monitoring and Diagnosis. *Sensors (Basel).* 2019;19(9):2164. doi:10.3390/s19092164
178. Chin SO, Keum C, Woo J, et al. Successful weight reduction and maintenance by using a smartphone application in those with overweight and obesity. *Sci Rep.* 2016;6:34563. doi:10.1038/srep34563
179. Chen J, Cade JE, Allman-Farinelli M. The Most Popular Smartphone Apps for Weight Loss: A Quality Assessment. *JMIR Mhealth Uhealth.* 2015;3(4):e104. doi:10.2196/mhealth.4334
180. Cai X, Qiu S, Luo D, Wang L, Lu Y, Li M. Mobile Application Interventions and Weight Loss in Type 2 Diabetes: A Meta-Analysis. *Obesity.* 2020;28(3):502-509. doi:10.1002/oby.22715
181. Wong MC, Ng BK, Kennedy SF, et al. Children and Adolescents' Anthropometrics Body Composition from 3-D Optical Surface Scans. *Obesity (Silver Spring).* 2019;27(11):1738-1749. doi:10.1002/oby.22637
182. Tian IY, Ng BK, Wong MC, et al. Predicting 3D Body Shape and Body Composition from Conventional 2D Photography. *Med Phys.* 2020;47(12):6232-6245. doi:10.1002/mp.14492
183. Tinsley GM, Moore ML, Dellinger JR, Adamson BT, Benavides ML. Digital anthropometry via three-dimensional optical scanning: evaluation of four commercially available systems. *Eur J Clin Nutr.* 2020;74(7):1054-1064. doi:10.1038/s41430-019-0526-6
184. Bourgeois B, Ng BK, Latimer D, et al. Clinically applicable optical imaging technology for body size and shape analysis: comparison of systems differing in design. *Eur J Clin Nutr.* 2017;71(11):1329-1335. doi:10.1038/ejcn.2017.142

185. Smith B, Dechenaud M, Heymsfield SB. Anthropometric Evaluation of a 3D Scanning Mobile Application. In: *Proceedings of 3DBODY.TECH 2021 - 12th International Conference and Exhibition on 3D Body Scanning and Processing Technologies, Lugano, Switzerland, 19-20 October 2021*. Hometrica Consulting - Dr. Nicola D'Apuzzo; 2021. doi:10.15221/21.33
186. Nana A, Staynor JMD, Arlai S, El-Sallam A, Dhungel N, Smith MK. Agreement of anthropometric and body composition measures predicted from 2D smartphone images and body impedance scales with criterion methods. *Obesity Research & Clinical Practice*. 2022;16(1):37-43. doi:10.1016/j.orcp.2021.12.006
187. Neufeld EV, Seltzer RA, Sazzad T, Dolezal BA. A Multidomain Approach to Assessing the Convergent and Concurrent Validity of a Mobile Application When Compared to Conventional Methods of Determining Body Composition. *Sensors (Basel)*. 2020;20(21):E6165. doi:10.3390/s20216165
188. Bosy-Westphal A, Booke CA, Blöcker T, et al. Measurement Site for Waist Circumference Affects Its Accuracy As an Index of Visceral and Abdominal Subcutaneous Fat in a Caucasian Population. *The Journal of Nutrition*. 2010;140(5):954-961. doi:10.3945/jn.109.118737
189. Graybeal A, Brandner C, Willis J. The Use of Smartphone-Based Artificial Intelligence to Predict Waist and Hip Circumference: A Physical Circumference Comparison. *Journal of the Academy of Nutrition and Dietetics*. 2022;122(9, Supplement):A46. doi:10.1016/j.jand.2022.06.226
190. Graybeal AJ, Brandner CF, Tinsley GM. Visual body composition assessment methods: A 4-compartment model comparison of smartphone-based artificial intelligence for body composition estimation in healthy adults. *Clinical Nutrition*. 2022;41(11):2464-2472. doi:10.1016/j.clnu.2022.09.014
191. Whelton PK, Carey RM, Aronow WS, et al. 2017 ACC/AHA/AAPA/ABC/ACPM/AGS/APhA/ASH/ASPC/NMA/PCNA Guideline for the Prevention, Detection, Evaluation, and Management of High Blood Pressure in Adults: A Report of the American College of Cardiology/American Heart Association Task Force on Clinical Practice Guidelines. *Hypertension*. 2018;71(6):e13-e115. doi:10.1161/HYP.0000000000000065
192. Gurka MJ, Lilly CL, Oliver MN, DeBoer MD. An examination of sex and racial/ethnic differences in the metabolic syndrome among adults: A confirmatory factor analysis and a resulting continuous severity score. *Metabolism*. 2014;63(2):218-225. doi:10.1016/j.metabol.2013.10.006
193. Lang PO, Trivalle C, Vogel T, Proust J, Papazian JP. Markers of metabolic and cardiovascular health in adults: Comparative analysis of DEXA-based body composition components and BMI categories. *Journal of Cardiology*. 2015;65(1):42-49. doi:10.1016/j.jjcc.2014.03.010

194. Lee BJ, Yim MH. Comparison of anthropometric and body composition indices in the identification of metabolic risk factors. *Sci Rep.* 2021;11(1):9931. doi:10.1038/s41598-021-89422-x
195. Sedlmeier AM, Baumeister SE, Weber A, et al. Relation of body fat mass and fat-free mass to total mortality: results from 7 prospective cohort studies. *Am J Clin Nutr.* 2021;113(3):639-646. doi:10.1093/ajcn/nqaa339
196. Romero-Corral A, Somers VK, Sierra-Johnson J, et al. Normal weight obesity: A risk factor for cardiometabolic dysregulation and cardiovascular mortality. *European Heart Journal.* 2010;31(6):737-746. doi:10.1093/eurheartj/ehp487
197. Sagun G, Oguz A, Karagoz E, Filizer AT, Tamer G, Mesci B. Application of alternative anthropometric measurements to predict metabolic syndrome. *Clinics (Sao Paulo).* 2014;69(5):347-353. doi:10.6061/clinics/2014(05)09
198. Janiszewski PM, Saunders TJ, Ross R. Breast Volume is an Independent Predictor of Visceral and Ectopic Fat in Premenopausal Women. *Obesity.* 2010;18(6):1183-1187. doi:10.1038/oby.2009.336
199. Yang Y, Xie M, Yuan S, et al. Sex differences in the associations between adiposity distribution and cardiometabolic risk factors in overweight or obese individuals: a cross-sectional study. *BMC Public Health.* 2021;21(1):1232. doi:10.1186/s12889-021-11316-4
200. Lee JJ, Pedley A, Therkelsen KE, et al. Upper body subcutaneous fat is associated with cardiometabolic risk factors. *Am J Med.* 2017;130(8):958-966.e1. doi:10.1016/j.amjmed.2017.01.044
201. Schorr M, Dichtel LE, Gerweck AV, et al. Sex differences in body composition and association with cardiometabolic risk. *Biology of Sex Differences.* 2018;9(1):28. doi:10.1186/s13293-018-0189-3
202. Flint AC, Conell C, Ren X, et al. Effect of Systolic and Diastolic Blood Pressure on Cardiovascular Outcomes. *New England Journal of Medicine.* 2019;381(3):243-251. doi:10.1056/NEJMoal803180
203. Miller M, Stone NJ, Ballantyne C, et al. Triglycerides and Cardiovascular Disease. *Circulation.* 2011;123(20):2292-2333. doi:10.1161/CIR.0b013e3182160726
204. Bandeali S, Farmer J. High-density lipoprotein and atherosclerosis: the role of antioxidant activity. *Curr Atheroscler Rep.* 2012;14(2):101-107. doi:10.1007/s11883-012-0235-2
205. Cho KH. The Current Status of Research on High-Density Lipoproteins (HDL): A Paradigm Shift from HDL Quantity to HDL Quality and HDL Functionality.

*International Journal of Molecular Sciences*. 2022;23(7):3967.  
doi:10.3390/ijms23073967

206. Graybeal AJ, Brandner CF, Tinsley GM. Validity and reliability of a mobile digital imaging analysis trained by a four-compartment model. *J Hum Nutr Diet*. Published online November 30, 2022. doi:10.1111/jhn.13113